Sustainable Technologies
EVALUATION PROGRAM

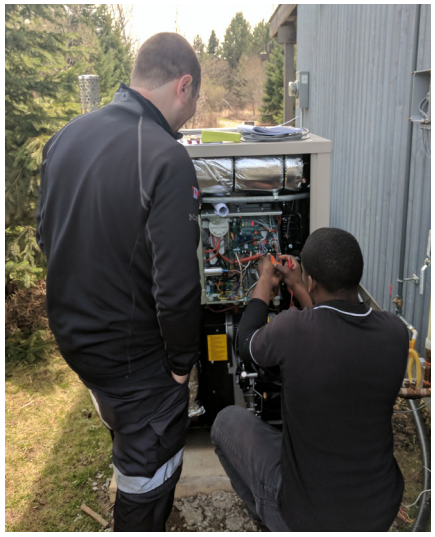


Gas Absorption Heat Pumps: Carbon, Energy and Cost Reductions for Heating Applications in a Cold Climate

Prepared by:
Toronto and Region Conservation Authority (TRCA)

January 2019

www.sustainabletechnologies.ca

PUBLICATION INFORMATION

Citation: Toronto and Region Conservation Authority (TRCA). 2019. *Gas Absorption Heat Pumps: Carbon, Energy and Cost Reductions for Heating Applications in a Cold Climate*. Toronto and Region Conservation Authority, Vaughan, Ontario.

Documents prepared by the Sustainable Technologies Evaluation Program (STEP) are available at www.sustainabletechnologies.ca. For more information about this or other STEP publications, please contact:

Leigh St. Hilaire
Project Manager II, STEP
Toronto and Region Conservation Authority
101 Exchange Avenue
Vaughan, Ontario
E-mail: lsthilaire@trca.on.ca

Erik Janssen
Analyst, STEP
Toronto and Region Conservation Authority
101 Exchange Avenue
Vaughan, Ontario
E-mail: ejanssen@trca.on.ca

THE SUSTAINABLE TECHNOLOGIES EVALUATION PROGRAM

The Sustainable Technologies Evaluation Program (STEP) is a multi-agency initiative developed to support broader implementation of sustainable technologies and practices within a Canadian context. STEP works to achieve this overarching objective by:

- Carrying out research, monitoring and evaluation of clean water and low carbon technologies;
- Assessing technology implementation barriers and opportunities;
- Developing supporting tools, guidelines and policies;
- Delivering education and training programs;
- Advocating for effective sustainable technologies; and
- Collaborating with academic and industry partners through our Living Labs and other initiatives.

Technologies evaluated under STEP are not limited to physical devices or products; they may also include preventative measures, implementation protocols, alternative urban site designs, and other innovative practices that help create more sustainable and livable communities.

ACKNOWLEDGEMENTS

Support for this project was provided by The Atmospheric Fund (TAF), Enbridge Gas Distribution Inc. and Union Gas Limited. This project was conducted in partnership with the research team of Dr. Alan Fung from the Ryerson University Department of Mechanical Engineering and Union Gas Limited. Additional funding support was provided by the City of Toronto, York Region and the Region of Peel. The research team would also like to acknowledge the valuable feedback and guidance provided by those who participated in the stakeholder advisory committee meetings for this project.

PROJECT TEAM

- Erik Janssen, Analyst, Sustainable Technologies Evaluation Program
- Aidan Brookson, Analyst, Sustainable Technologies Evaluation Program
- Gil Amdurski, Technical Coordinator, Sustainable Technologies Evaluation Program
- Leigh St. Hilaire , Project Manager II, Sustainable Technologies Evaluation Program
- David Nixon, Advisor, Sustainable Technologies Evaluation Program
- Ricardo Brown, Monitoring Technician, Sustainable Technologies Evaluation Program
- Amanda Yip, Project Coordinator, Sustainable Technologies Evaluation Program
- Alan Fung, Associate Professor, Ryerson University
- Rakesh Kumar, Senior Energy Systems Researcher, Ryerson University
- Kajen Ethirveerasingham, Master's Student, Ryerson University
- Altamash Ahmad Baig, PhD Candidate, Ryerson University
- Navid Ekrami, Research Engineer, Ryerson University
- Kai Ye, Undergraduate Student, Ryerson University
- Ahmad Mhanna, Undergraduate Student, Ryerson University
- Monica Brands, Undergraduate Student, Ryerson University

NOTICE

The contents of this report do not necessarily represent the policies of the supporting agencies. Although every reasonable effort has been made to ensure the integrity of the report, the supporting agencies do not make any warranty or representation, expressed or implied, with respect to the accuracy or completeness of the information contained herein. Mention of trade names or commercial products does not constitute endorsement or recommendation of those products.

EXECUTIVE SUMMARY

Introduction

Buildings are a major source of carbon emissions in Canada. Most of these emissions are attributable to the natural gas used for space heating. High-efficiency versions of standard heating equipment may help reduce emissions but they cannot surpass 100% efficiency. Alternatively, heat pump technologies achieve efficiencies that are beyond the conventional limit because they supplement the energy contained in a fuel (i.e. gas or electricity) with heat energy extracted from the air, ground or elsewhere, making deeper carbon reductions possible. Gas heat pumps (GHPs) have been successfully applied in Europe and Japan, but have not made significant inroads in Canada and their cold-climate operation has not been thoroughly studied. This project analyzed the operation of an air-to-water gas absorption heat pump installed at the Archetype Sustainable House (ASH) Lab in Vaughan, Ontario, during 2017-18.

Technology

The heat pump was the GAHP-AR from Robur (Figure A). It is a gas-driven air-to-water heat pump that provides both heating and cooling. Rated heating capacity and efficiency are 35.3 kW and 126% (HHV), respectively, and the unit can supply fluid up to a temperature of 60 °C. A non-reversible version of the technology (GAHP-A) is also available. The unit is a single package installed outdoors, on a pad or rooftop, and connected to a building via hydronics. The capacity of the heat pump makes it well-suited to large homes, multi-unit residential and industrial-commercial-institutional (ICI) sectors.

Figure A. The GHP installed outdoors.

Study Site

The ASH Lab consists of two semi-detached LEED platinum homes. It is uniquely equipped with a state-of-the-art control and data acquisition system and has been used in dozens of academic and industry research projects. The Lab was used in conjunction with variable auxiliary coils to load the GHP to desired levels during testing. Note that, while the ASH Lab provided a heating load for the GHP, the testing was designed to produce generalized results that are applicable to different building types.

Figure B. The ASH Lab was used as a load.

Heating Mode Results

Experimental testing generated performance maps characterizing the impact of various parameters on performance. Measured steady-state heating mode capacity and efficiency, as a function of outdoor temperature and inlet fluid temperature (indicated by the different colours), are shown in Figures C. Note that the efficiency plots for both heating and cooling mode consider gas consumption, while the electricity consumption was taken into account when determining overall savings.

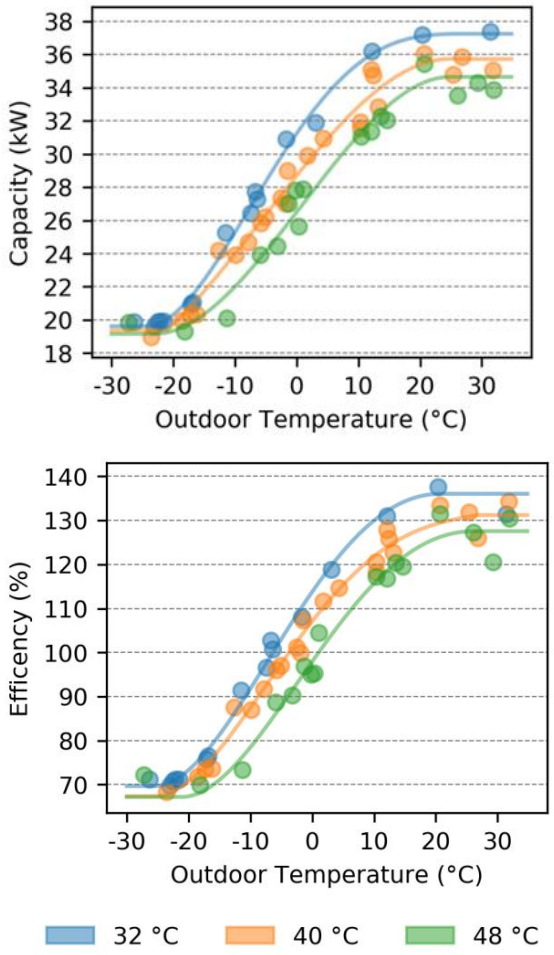

Figure C. GHP heating capacity (top) and gas efficiency (bottom) for different ambient outdoor temperatures and inlet fluid temperatures.

Cooling Mode Results

Similar performance maps were generated for cooling mode. Efficiency is plotted in Figure D. It was found that the low cooling mode efficiency would result in notably greater emissions when compared to electric cooling. For smaller applications that do not pay electrical demand charges, cooling mode utility costs associated with the GHP would also be greater. However, cost implications are complex for larger applications because increased 'per-unit' utility costs could be offset by decreased electrical demand charges. This was not explored in detail within this study. However, as a cost-effective low-carbon technology, the non-reversible version of the technology (GAHP-A) is preferred in Canada and only heating mode was considered in the annual performance projections.

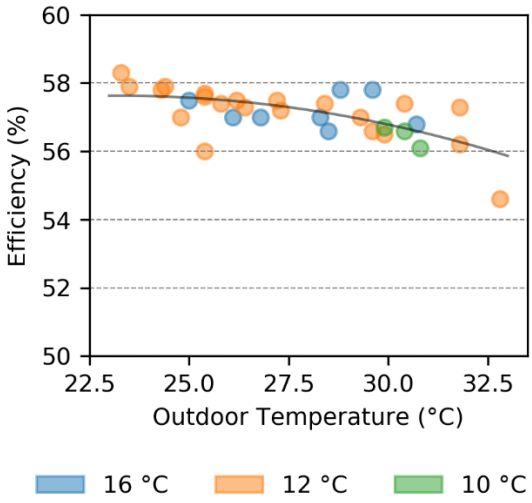

Figure D. GHP cooling capacity (top) and efficiency (bottom) for different ambient outdoor temperatures and inlet fluid temperatures.

Cycling Results

Figures C and D ignore start-up losses. The impact of these losses on performance depend on the duration of time that the GHP turns on

when responding to a heating call (termed 'cycle time'). Cycling losses with respect to cycle time are shown in Figure E. At 40 min, the derate factor is 0.92. This means that actual efficiency for the cycle is 8% lower than the steady-state value shown in Figure C. It is clear that longer cycle times are critical for high performance and this should be promoted through system design and control.

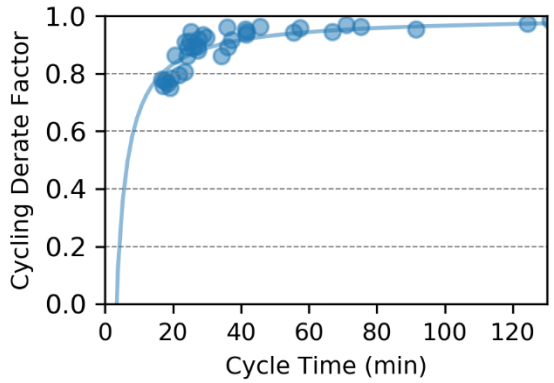

Figure E. GHP cycle derate factor.

Annual Performance Projections

In the context of an hourly bin analysis, the heating mode performance maps were used to estimate annual savings versus a high-efficiency boiler (with an assumed real-world efficiency of 88%). Results from different scenarios are in Figure F and G. Cycling derates were neglected because the cycle time is a dynamic factor specific to individual installations and operating conditions. The results are therefore an upper limit of potential savings. Note that net savings take into account both gas reductions and electrical consumption increases (the unit consumed ~1 kW of electricity during normal operation).

DHW-PH assumed that a GHP was used for domestic hot water (DHW) pre-heat with a larger boiler. *DHW* assumed that the GHP replaced a DHW boiler. *SH-48*, *SH-40* and *SH-32*, assumed space-heating loads with a 48, 40 or 32 ˚C inlet temperature, respectively. It is clear that DHW pre-heating is an ideal application. It exploits many factors contributing to a high-efficiency, such as lower inlet temperatures, warmer outdoor ambient conditions, greater operating hours, and even reduced cycling losses. Note that cost results are highly sensitive to the utility rates. For simplicity, this study used estimates of current rates for small-to-medium consumers and did not consider all applicable rates or cost escalation. Prospective system owners are encouraged to consider the impacts of their rates on the findings the study.

Business Case

Annual net cost savings for DHW pre-heating applications were projected to be ~$1,500 in Toronto, neglecting any incentives, rebates or carbon pricing. Carbon savings for this application were substantial, at 16 tons CO_2e per year. If the heat pump can benefit from carbon pricing, then annual savings could increase to $2,300 per year. The current list price (Oct. 2018) for the non-reversible version of the technology is approximately $21,000 (although prices will vary). Note that the market for this technology in Canada is not mature and prices may come down as uptake increases. High-efficiency condensing gas boilers sold by the same distributor have a list price of approximately $6,500. The incremental capital cost was then estimated at $14,500. It follows that a 6- to 10-year payback is feasible for this application.

Implementation

The GHP operated without issue during testing and it did not require any special expertise beyond that for natural gas boilers.

Conclusion

It is important to note that the approach used in this study was sufficient to identify the applications and locations where the unit is best applied, as well as provide projections for savings. However, the authors acknowledge that additional work is needed to fully evaluate, in detail, the benefits for specific applications. In general, gas absorption heat pumps are a promising technology for carbon reduction. This study showed that, while it is not a cost-effective replacement for conventional gas heating technologies in *every* instance due to the high capital cost and electrical power consumption, DHW applications have strong potential for notable operational cost and carbon reductions.

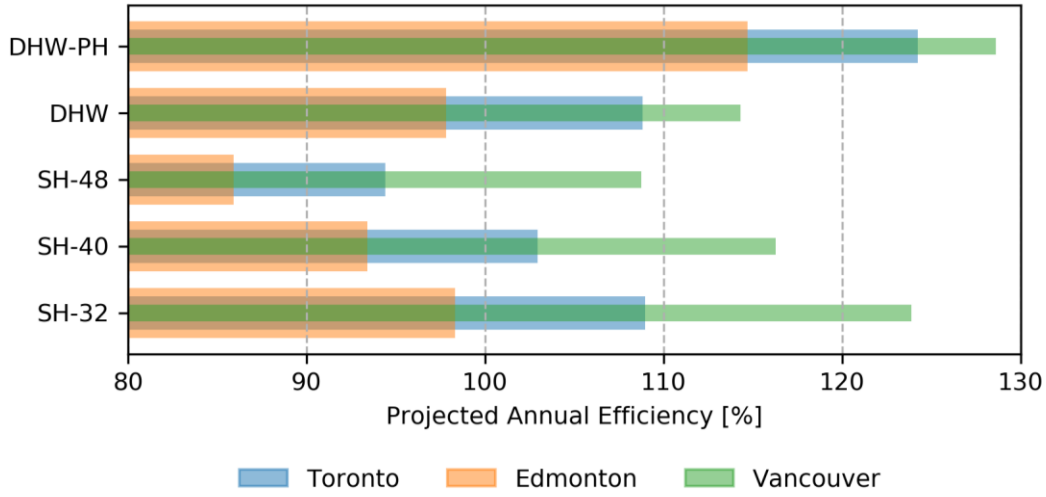

Figure F. Projected annual efficiency (based on HHV) for the different scenarios considered in this study.

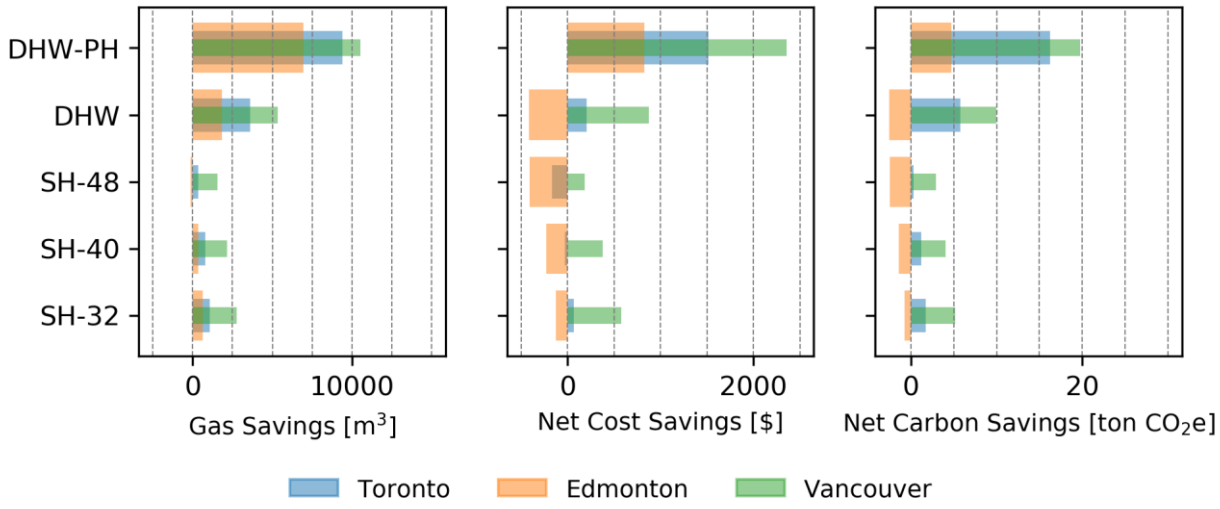

Figure G. Projected annual savings for the different scenarios considered in this study.

CONTENTS

1.0 INTRODUCTION

Buildings are a major source of carbon emissions in Canada. The majority of emissions within the sector are attributable to the combustion of natural gas used for space heating. High-efficiency natural gas heating technology may be used to reduce gas consumption, but any conventional technology will be limited by an efficiency that cannot exceed 100%. More advanced technology is required to achieve deeper carbon reductions while still utilizing inexpensive natural gas as a fuel.

Heat pump technology achieves efficiencies that are beyond the conventional limit because the energy contained in a fuel (i.e. gas or electricity) is supplemented with heat energy extracted from the air, ground or elsewhere. It follows that a heat pump can deliver more heat energy to a building than is contained in a fuel and have an "efficiency" that is greater than 100%[1]. Heat pumps may also provide cooling.

Electrically driven heat pumps are more efficient than natural gas heat pumps (GHPs) by a wide margin but electricity is a higher grade of energy with a much higher cost *per unit* energy when compared with natural gas (at 2018 prices in the Canadian jurisdictions considered in this study). It follows that, although an electric heat pump is several times more efficient than conventional gas heating equipment, it does not actually cost less to operate in many applications.

GHPs are much more efficient than conventional gas heating equipment. The key benefit of GHPs is that they achieve a high efficiency, albeit still much lower than electric heat pumps, while still utilizing a low-cost fuel. This holds promise for a better business case and for achieving deeper carbon reductions in the short-term. GHPs have been successfully applied in Europe and Japan, but have not made significant inroads into the Canadian market and their operation in a cold-climate has not been thoroughly studied.

This project analyzed the operation of an air-to-water gas absorption heat pump installed at the Archetype Sustainable House (ASH) Lab in Vaughan, Ontario, over the 2017 cooling season and 2017/2018 heating season. The primary goal of the research was to create a detailed map of the heat pump's performance across the range of outdoor conditions experienced in a Canadian climate such that energy, cost and carbon reductions associated with the GHP could be estimated.

[1] Here "efficiency" is defined as the heat energy delivered to the space divided by the heat energy contained in the fuel that was consumed.

2.0 BACKGROUND

2.1 Principle of Operation

A schematic of the gas absorption heat pump cycle is presented in Figure 2-1, and the process is described below.

- The generator contains a solution of ammonia and water. Heat from natural gas combustion is applied to the generator, ammonia gas boils out of the solution and water is recirculated.
- The hot ammonia gas has a high energy content because of the latent heat of evaporation. It condenses into a liquid at the condenser and releases its heat.
- The expansion valve reduces the pressure of the system, allowing the ammonia to boil at a lower temperature. Heat energy, available at a low-temperature, from the outside air (or ground), is absorbed in the evaporator. This boils the ammonia.
- The low-pressure low-temperature ammonia gas is recombined into an ammonia-water solution at the absorber. The solution is then pumped back to the generator.

The heat rejected at the condenser is equal to the heat absorbed at the evaporator plus the heat applied to the generator. In this way, the GHP is able to extract renewable heat energy from the air or ground to supplement the heat energy released from natural gas combustion. Some heat pump units will also operate the cycle in reverse to provide cooling.

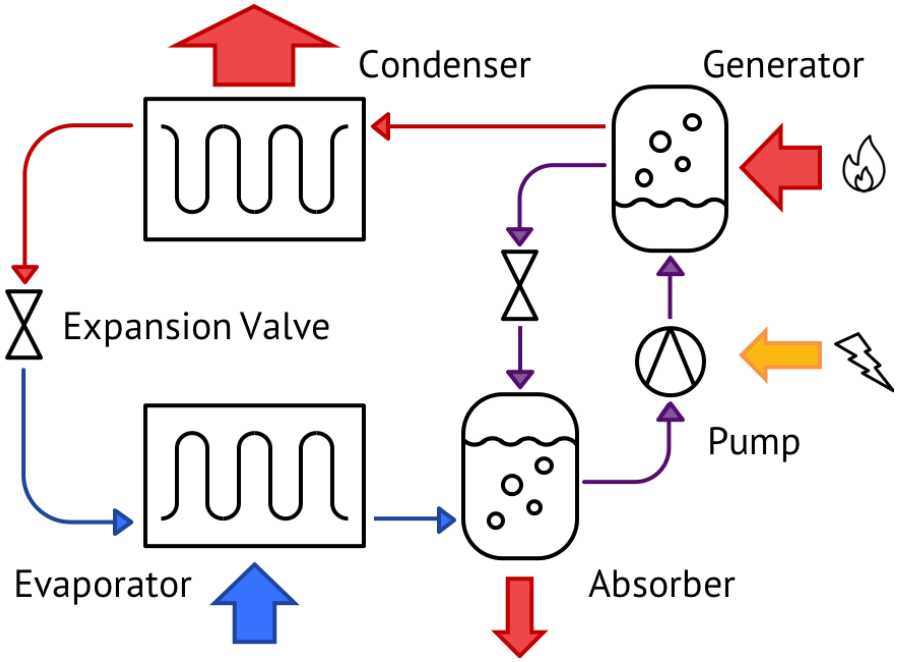

Figure 2-1. Schematic of the absorption heat pump cycle.

2.2 GHP

The heat pump under study in this project was the GAHP-AR from Robur (Figure 2-2). It is a reversible air-to-water heat pump that can provide both heating and cooling (alternately but not simultaneously). A non-reversible version of the technology is also available (GAHP-A). All heat pump components are housed in a single package that is installed outdoors, on a pad or rooftop, and connected to a building via hydronics. The unit is single speed and therefore does not modulate its capacity output. Specifications are shown in Table 2-1.

Figure 2-2. GHP installed on a pad at the ASH Lab.

The capacity of the GHP makes it well suited to large single-family dwellings, as well as the multi-unit residential (MURB) or industrial-commercial-institutional (ICI) sectors. Example buildings in this sector would include: offices, retail, restaurants, hotels, nursing homes, schools, university/colleges, warehouses, apartments, etc. The GHP is also scalable. Multiple units can operate together as a heating and cooling plant, coordinated by the direct digital controller (DDC) option available for the system.

Table 2-1. GHP specifications.

Parameter	Value
Heating	
Heating Capacity	120,400 Btu/hr (35.3 kW)
Gas Input (HHV)	95,500 Btu/hr (28.0 kW)
Efficiency (HHV)	126%
Minimum Ambient Operating Temperature	-20 ˚C
Maximum Outlet Water Temperature	60 ˚C
Nominal Flow Rate (GPM)	13.4 GPM
Cooling	
Cooling Capacity	57,700 Btu/hr (16.9 kW)
Gas Input (HHV)	95,500 Btu/hr (28.0 kW)
Cooling Efficiency (HHV)	60%
Maximum Ambient Operating Temperature	45 ˚C
Minimum Outlet Water Temperature	3 ˚C
Nominal Flow Rate	12.8 GPM
Electrical	
Power Consumption	0.9o/0.93 kW (Depends on version)
Physical Data	
Weight	838 lbs
Dimensions	33.5 x 48.5 x 50.75 in (W x L x H)

Manufacturer specifications indicate the capacity and efficiency when using water as the heat transfer fluid with an inlet temperature of 40 ˚C (outlet at 50 ˚C) and an ambient outdoor temperature of 7 ˚C. In a cold Canadian climate, temperatures will frequently be much colder than the nominal operating point and an antifreeze heat transfer fluid, like propylene glycol, is required to prevent freezing at cold temperatures during periods of low load or when the heat pump is idle. A 50% propylene glycol

solution was used in this study and it prevents freezing down to -34 ˚C. Temperatures as cold as -27 ˚C were observed during the testing. Propylene glycol has poorer heat transfer properties than water and this will degrade both the efficiency and capacity of the unit. The data is incomplete on how propylene glycol will affect performance in heating mode. A discussion of this topic is provided in Appendix A.

3.0 STUDY SITE

The Sustainable Technologies Evaluation Program (STEP) operates many real-world laboratories to evaluate low-carbon technologies and most of these are located at the Kortright Centre for Conservation in Vaughan, ON. The Archetype Sustainable House (ASH) Lab at Kortright (Figure 3-1) is used by STEP and its partners to evaluate and demonstrate renewable energy, HVAC, building science and energy efficiency technologies and designs for the residential market. The ASH was constructed in 2009 and consists of two semi-detached 3-story LEED platinum houses, termed House A (to the right of the image) and House B (to the left). It is uniquely instrumented with a state-of-the-art data acquisition and control system to monitor and implement different technologies, and has been used as the testing environment for dozens of academic and industry research projects.

Figure 3-1. The Archetype Sustainable House (ASH) Lab is used to demonstrate and research low-carbon technologies for the residential market.

The ASH Lab served as a convenient study site but the GHP had more capacity than was required. Additional variable auxiliary load and thermal storage capacity were added. The auxiliary load was implemented using a set of two outdoor fan units with hydronic coils (Figure 3-2) that were connected in series with the primary hydronic loop of the ASH. During testing, the auxiliary load fan speeds were controlled manually using a variable transformer. To increase the thermal storage capacity of the ASH, two 300L storage tanks were added to the existing 270 L buffer tank used for the house HVAC system.

The auxiliary load and thermal storage were used to make the ASH behave thermally like a much larger building, such that when the GHP turned-on it had an adequate amount of load. This mitigated issues surrounding short-cycling during some periods of data collection. The auxiliary load was also used to manually trim the return temperature to precise values, allowing the research team to

accurately map performance as a function of the glycol return temperature, as well as outdoor temperature, when operating in steady-state.

Figure 3-2. Fan coil auxiliary load.

A high-level diagram of the hydronic system of the ASH Lab is shown in Figure 3-3. The GHP was connected to the same primary hydronic loop as House A, House B and the auxiliary load. The House A distribution system was forced-air and the House B distribution system was radiant in-floor. Heated glycol from the GHP flowed directly through a hydronic heating coil in the House A air handler but it was interfaced to buffer tanks in House B using a parallel plate heat exchanger. The glycol flowed through the auxiliary loads before returning to the GHP.

The installation used low-cost PEX piping and did not require any unique fittings or components that would not also be required in a more conventional hydronic heating system; nor were there any installation challenges beyond that of conventional hydronic heating systems. Aside from the gas connections and GHP commissioning, the system was designed and installed by STEP personnel with help from Ryerson University.

It is important to note that the actual distribution systems of House A and House B are less important and are not discussed in detail here. In the context of this study, it is sufficient to think of House A and B simply as spaces to reject heat. Study results would have been comparable had different loads been used.

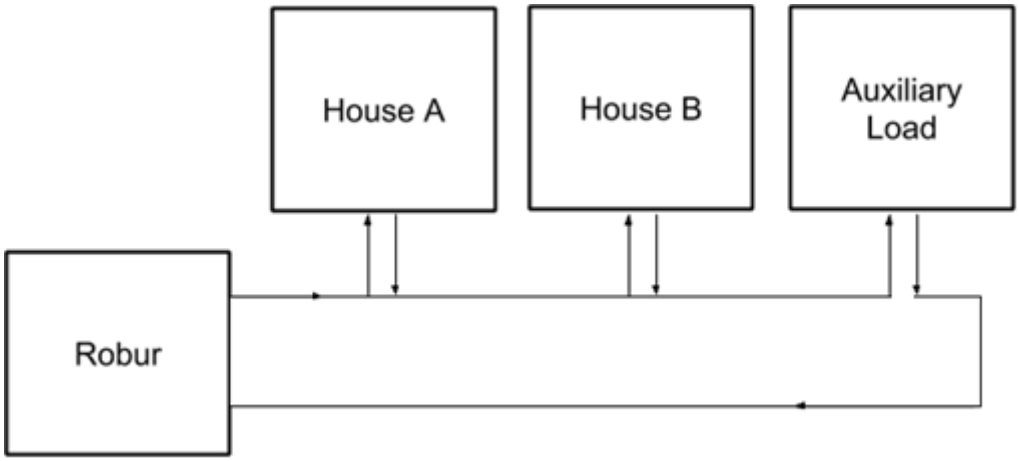

Figure 3-3. Schematic of hydronic system.

4.0 INSTRUMENTATION

Hydronic flow and temperature monitoring points are shown in Figure 4-1. There was sufficient data collection to determine the heat energy supplied by the GHP and also that which was delivered to each load in the system. Other monitoring points included: gas consumption of the GHP, power consumption of the GHP, power consumption of the primary circulator, outdoor temperature and outdoor relative humidity.

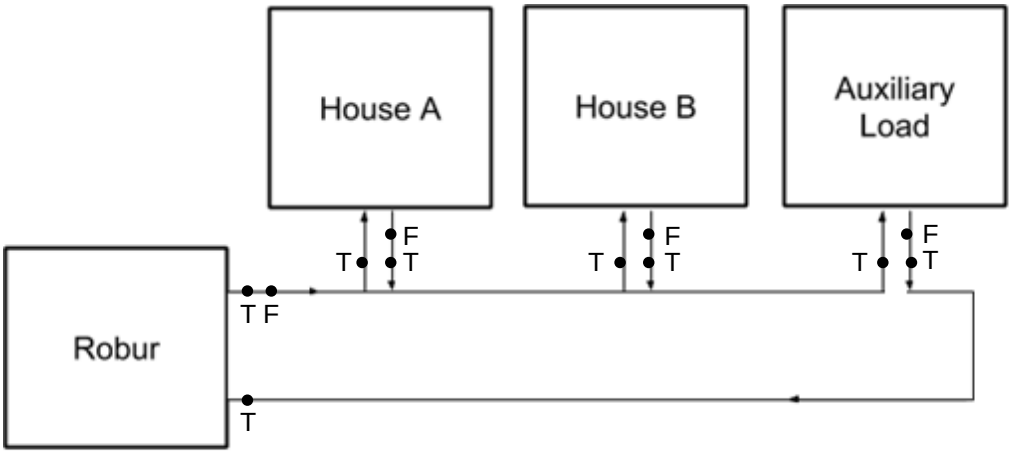

Figure 4-1. Hydronic system monitoring points.

A summary of the sensors used for each monitoring point is given in Table 4-1. Sensors were calibrated or verified at the ASH lab prior to deployment for this study. Flow sensors were verified using a custom set-up where flow meters measured water flowing into a tank of known volume. Temperature sensors were calibrated as matched-pairs using a wet-well temperature calibrator. Ambient environmental measurements were compared against instrumentation already installed on site. Measurements from the pulse-output gas meter were verified using manual readings from the existing whole-house gas meter. Electrical measurements were verified using a calibrated electrical power meter.

All sensors were connected with the existing ASH Lab acquisition system based on the Compact Field Point (cFP) topology from National Instruments. Data acquisition was coordinated by a custom program in LabView at a logging interval of 5 s. Pictures of the mounting for certain key sensors is shown in Figure 4-2 to Figure 4-5, including the GHP supply and return temperature sensors, the primary loop flow meter, the outdoor temperature/humidity sensor and the gas meter.

Table 4-1. Description of sensors.

	Description/ Location	Sensor	Sensor Output	Expected Accuracy
Heating and Cooling to House A	House A Flow	MAG-VIEW magnetic flow meter from Mass Flow Online	Pulse	± 2%.
	House A Supply Temp.	Pt500 RTD from Kamstrup	Resistance	±0.2 ˚C.
	House A Return Temp.	Pt500 RTD from Kamstrup	Resistance	±0.2 ˚C.
Heating and Cooling to House B	House B Flow	MAG-VIEW magnetic flow meter from Mass Flow Online	Pulse	± 2%.
	House B Supply Temp.	Pt500 RTD from Kamstrup	Resistance	±0.2 ˚C.
	House B Return Temp.	Pt500 RTD from Kamstrup	Resistance	±0.2 ˚C.
Heating and Cooling from GHP	GHP Flow	MAG-VIEW magnetic flow meter from Mass Flow Online	Pulse	± 2%.
	GHP Supply Temp.	Pt500 RTD from Kamstrup	Resistance	±0.2 ˚C.
	GHP Return Temp.	Pt500 RTD from Kamstrup	Resistance	±0.2 ˚C.
Heating and Cooling to Aux. Load	Dump Load Flow	MAG-VIEW magnetic flow meter from Mass Flow Online	Pulse	± 2%.
	Dump Load Supply Temp.	Pt500 RTD from Kamstrup	Resistance	±0.2 ˚C.
	Dump Load Return Temp.	Pt500 RTD from Kamstrup	Resistance	±0.2 ˚C.
Energy Inputs	Gas Flow	Elster American Diaphragm Meter 52142G014	Pulse	± 2%.
	GHP Power Consumption	Wattnode from Continental Control Systems	Pulse	±2 %.
	Primary Loop Circulator(s) Power Consumption	Wattnode from Continental Control Systems	Pulse	±2 %.
Outdoor Conditions	Outdoor Ambient Temp.	HMS82 Outdoor Humidity and Temperature Transmitter from Vaisala	4-20 mA	±0.2 ˚C.
	Outdoor Relative Humidity	HMS82 Outdoor Humidity and Temperature Transmitter from Vaisala	4-20 mA	±0.2 ˚C.

Figure 4-2. Supply and return temperature sensors were mounted as close to the unit as possible. They were mounted in thermal wells using a thermal grease and insulation was used to cover the thermal well.

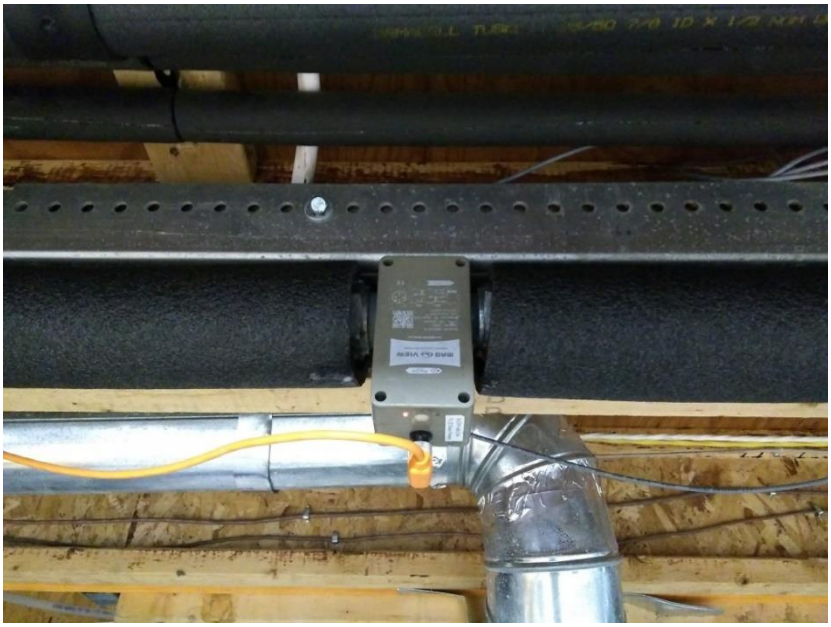

Figure 4-3. The primary loop magnetic flow meter was mounted in the basement of House B.

Figure 4-4. The outdoor ambient temperature and humidity sensor was installed with a radiation shield on the east side of the ASH roughly 12 ft (horizontally) from the GHP.

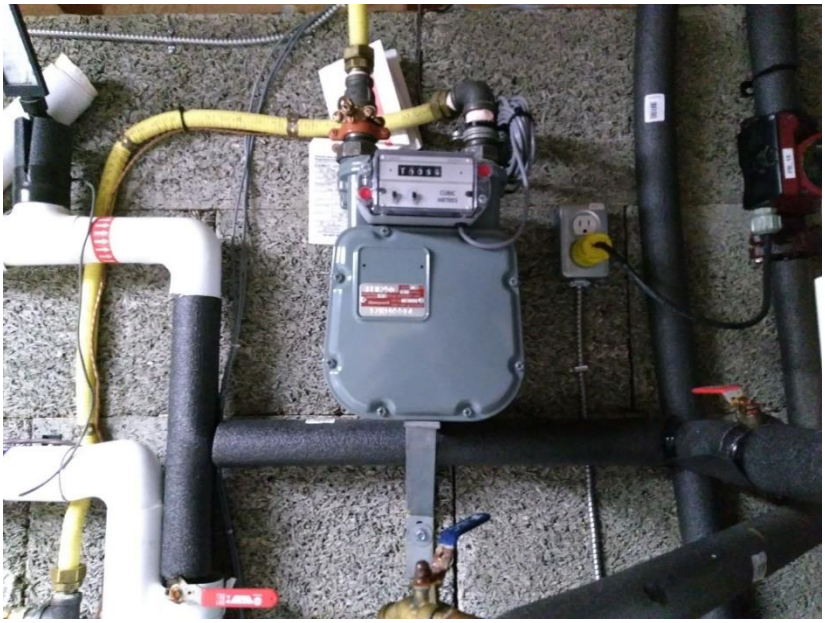

Figure 4-5. A dedicated gas submeter for the GHP was installed in the basement of House B.

5.0 CONTROL

The GHP was installed with a direct digital controller (DDC). The DDC was used as the interface to configure the unit. The control circuit was designed such that the GHP could be manually forced on or off using a toggle switch, or turn on or off based on heating or cooling calls from House A or House B. During certain parts of the testing the unit was simply forced on and during others, it was allowed to operate according to the heating or cooling requirements of the ASH Lab.

Figure 5-1. The DDC was used to input parameters for the GHP.

6.0 COMMISSIONING

Natural gas connections and commissioning of the GHP itself were performed by a licensed gas fitter according to the installation guidelines and commissioning checklist provided by the manufacturer. The gas fitter did not require any additional training or skills to connect and commission the unit. No faults codes or other issues were detected on start-up.

7.0 TESTING PLAN

The overall aim of the testing plan was to develop a performance map of the GHP in heating and cooling mode. The performance map defined the capacity and efficiency of the unit as a function of key parameters, including: outdoor ambient temperature, return glycol temperature, glycol flow rate and cycle time.[2] The performance map is a property of the GHP itself rather than this specific installation and, as such, it could be used to help estimate the performance of the unit in other buildings and applications. The testing plan incorporated two different types of testing: steady-state and cycling.

7.1 Steady-state Testing

The steady-state testing evaluated the performance of the GHP in the limit of very long cycle times and unvarying conditions. The aim of the steady-state testing was to empirically determine the effect of outdoor temperature, return temperature and flow rate, on the capacity and efficiency of the unit. The steady-state testing did not incorporate losses from start-up; these were included using data from the cycling testing portion of the monitoring.

During the planning stages of the project, the research team identified a matrix of desired operating conditions to evaluate during the steady-state testing. This is shown in Table 7-1. Performance data was desired across a continuous range outdoor temperatures occurring during *both* the heating and cooling season. The heating mode performance for warm outdoor temperatures was desired so as to estimate the performance of the unit when used for domestic hot water (DHW), which is needed throughout the year and not just during colder months.

Three different return temperatures were selected: 32, 40 and 48 ˚C. Note that, for design flow conditions, the supply temperature is approximately 10 ˚C higher than the return. These temperatures were selected to represent different applications towards which the GHP could be applied. The lower temperature represents low-temperature radiant heating applications, the medium temperature represents forced air applications and the higher temperature represents DHW applications or high-temperature heating.

A return temperature of 48 ˚C was selected as the warmest operating point that would still keep the unit from shutting itself off due to overheat protection, which occurred when the supply reached 60˚C.[3] At the other end of the range, 32 ˚C was selected as the lowest temperature operating point

[2] By "cycle time" it is meant the amount of time the unit stays on to provide heating or cooling once it initially turns on in response to a thermostat call.

[3] In practice, both the overheat and freeze protection limits of the GHP were met many times during operation and testing. In every case, the unit successfully turned itself off and was undamaged. Also note that the 60 ˚C overheat protection temperature could be problematic where higher temperatures are required.

because it was difficult to provide enough load such that the system would balance at a return of 32˚C, particularly under warmer outdoor conditions.

Table 7-1. Matrix of heating mode operating conditions during steady state testing.

		Outdoor Temperature [˚C]							
		-25	**-15**	**-5**	**0**	**5**	**15**	**25**	**35**
Return Temperature [˚C]	**32**	1	1	1	1	1	1	1	1
		2	2	2	2	2	2	2	2
		3	3	3	3	3	3	3	3
	40	1	1	1	1	1	1	1	1
		2	2	2	2	2	2	2	2
		3	3	3	3	3	3	3	3
	48	1	1	1	1	1	1	1	1
		2	2	2	2	2	2	2	2
		3	3	3	3	3	3	3	3

The values "1", "2", or "3", represent a pump speed setting; with "2" approaching the design flow recommendations, "1" being at the lower edge of the recommended flow range and "3" being at the upper edge. Flow rate was anticipated to have a smaller effect on performance and data near the design flow conditions was prioritized as being more important within the study.

Steady-state testing proceeded as follows:

- The team would monitor the short-term weather forecast to determine the outdoor temperatures that were likely to occur. These temperatures were cross-checked against the steady-state data that had already been collected and a decision was made on which operating conditions (of those outlined in Table 7-1) to select for testing.
- Prior to a test, a test operator would access the testing dashboard which provided real-time values for all data points, and real-time updating and historical plotting for the return glycol temperature (Figure 7-1). Test operators were either Ryerson students or STEP personnel. The dashboard provided key information about how the testing was progressing and if any changes were required to keep the system in a steady-state. It also confirmed that there was no erroneous data or problems with the data logging system.
- The GHP was manually forced on. Set-points or other parameters were adjusted in House A and House B to load the system to a point where the actual return temperature was near the desired value.
- The operator would then manually trim the return temperature to the desired value using the variable capacity auxiliary loads.

- The operator would record the time that system reached a steady-state, as well as any other relevant details about the testing conditions, and keep the system operating in a steady-state by adjusting the auxiliary loads for a duration of 45 minutes, or 30 minutes if 45 minutes was not possible.
- Data was logged at 5 second intervals. A STEP analyst visually inspected the testing data. Based on the testing times provided in the testing notes and visual inspection of the data, the steady-state data used for calculation purposes was selected from the overall data trend.
- Capacity and efficiency were then calculated for the selected range of steady-state data.

An example of steady-state data collected during a test is provided in Appendix B.

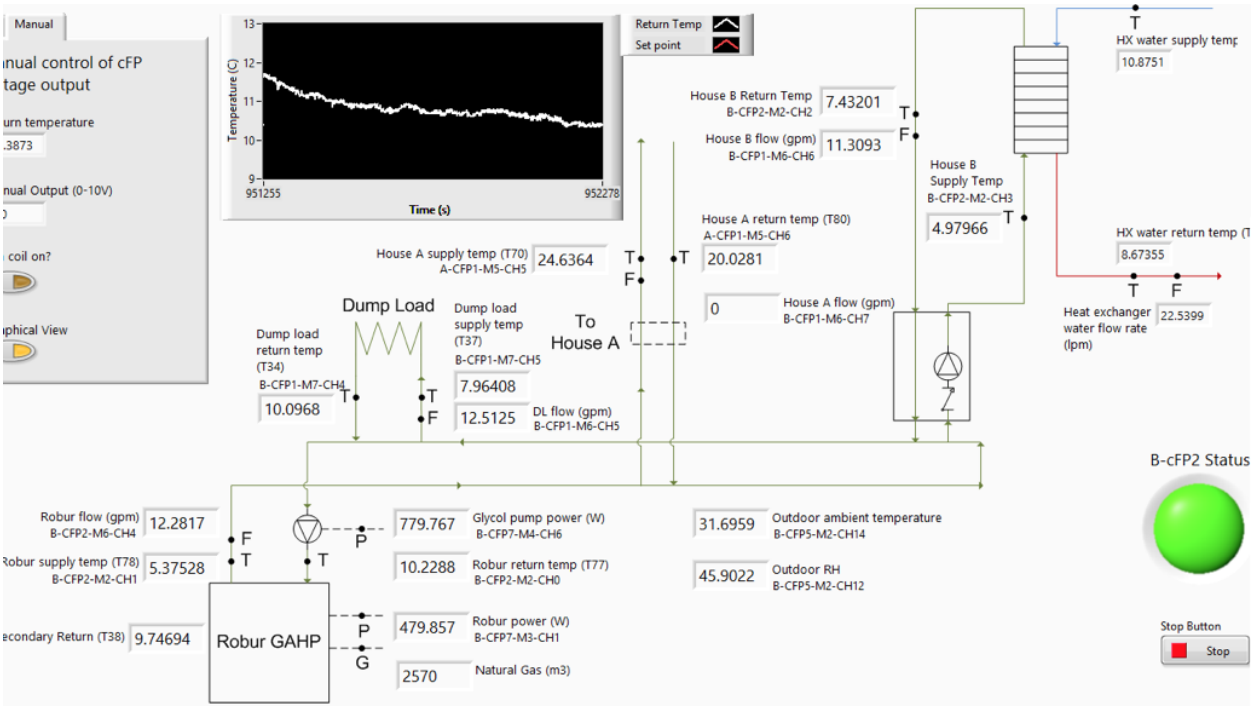

Figure 7-1. Screenshot of dashboard used by operator during steady-state testing.

It is worth noting that standardized performance testing of electric air-source heat pumps starts with a defrost cycle. The purpose of the defrost cycle is to remove any frost build-up on the coils that may negatively impact performance. The GHP has a propriety control algorithm for defrosting and it was not possible to manually trigger it if certain other conditions were not met. It follows that steady-state tests were not preceded by a defrost cycle. However, it should be noted that the GHP is different than an electric air-source heat pump because it appeared to almost never go into a defrost cycle. The DDC controller records the total number of defrost cycles and it only entered one defrost cycle during the entire heating season of 2017/2018. This information from the DDC is believed to be trustworthy, because at no point did the outdoor coil appear heavily frosted nor was there any physical evidence that a defrost cycle occurred (such as ice build-up under the coil).

Steady-state cooling testing proceeded in a similar way. The matrix of operating points for the steady-state cooling tests is shown in Table 7-2. The differential between supply and return in cooling mode under design flow conditions is 5 ˚C. Freeze protection initiates when the supply reaches 3 ˚C. The lowest return temperature was selected such that it could still operate in a steady-state without entering freeze protection. The highest return temperature of 16 ˚C required a large degree of loading from the system and it represented a value that was achievable for most outdoor temperatures considered.

Table 7-2. Matrix of steady-state operating points considered during cooling testing.

		Outdoor Temperature [˚C]				
		15	**20**	**25**	**30**	**35**
Return Temperature [˚C]	**16**	1	1	1	1	1
		2	2	2	2	2
		3	3	3	3	3
	12	1	1	1	1	1
		2	2	2	2	2
		3	3	3	3	3
	10	1	1	1	1	1
		2	2	2	2	2
		3	3	3	3	3

7.2 Cycling Testing

The *steady-state* performance map reflects the effect of different parameters on performance in the limit of long cycle times. The influence of start-up losses on overall efficiency, which depend on the cycling time, can be taken into account through an appropriate derate function applied to the performance map. During cycling testing, the GHP was used to meet the load of the ASH (with the auxiliary loads off or set at a constant value) as required by thermostat calls from the houses. The DAQ system logged in the background at a 5 second interval.

Individual cycles were extracted from the dataset and the total cycle efficiency was compared against the steady-state efficiency to calculate a performance derate. It was important that a variety of cycle times, both long and short, occurred during the cycle testing. Note that the overall performance of GHP at heating or cooling the ASH Lab was *not* calculated. The ASH was simply used a convenient testing platform and not intended to be representative of an actual installation.

8.0 TIMELINE

The design of the system and procurement of components began in December 2016. The system was commissioned, and instrumentation was installed and complete, in July 2017. Cooling mode data was collected primarily between July 2017 and September 2017, with some additional data collected during summer 2018. Heating mode data was collected between October 2017 and March 2018.

9.0 ANALYSIS

9.1 Steady-state Capacity and Efficiency

The capacity and efficiency of the GHP were calculated for each operating condition outlined in Table 7-1 and Table 7-2. Heating capacity ($\dot{q}_h$) is given in units kW within Equation 1, where:

- i is an index that represents a 5-second logging interval ($i = 1$ being the first logging interval in the steady-state period and $i = n$ being the last),
- $\dot{m}_i$ is the mass flow (in units of kg/s of the glycol through the GHP) as measured during the ith logging interval,
- C is the specific heat capacity of the glycol (in units kJ kg^{-1} °C^{-1}) calculated at the average of the supply and return temperatures for the ith logging interval,
- $T_{s,i}$ is the supply glycol temperature from the GHP during the ith logging interval, and
- $T_{r,i}$ is the return glycol temperature from the GHP during the ith logging interval.

$$\dot{q}_h = \frac{\sum_{i=1}^{n} \dot{m}_i \cdot C \cdot \left(T_{s,i} - T_{r,i}\right)}{n} \qquad \text{Equation 1}$$

Heating mode efficiency considering only the natural gas input ($\eta_{h,gas}$) is given in Equation 2, where:

- $\dot{q}_g$ is the average rate of gas energy consumption during the steady-state interval (in units kW),
- $\dot{V}_g$ is the gas volumetric flow (in units m^3/s),
- ε is the energy content of gas (in units kJ/m^3).

$$\eta_{h,gas} = \frac{\dot{q}_h}{\dot{q}_g} \qquad \text{Equation 2}$$

$$\dot{q}_g = \varepsilon \cdot \dot{V}_g \qquad \text{Equation 3}$$

Comparable calculations were conducted for cooling mode with the exceptions that the equations for $\dot{q}_c$ is slightly different than that for $\dot{q}_h$ (Equation 4) because supply and return temperatures are switched.

$$\dot{q}_c = \frac{\sum_{i=1}^{n} \dot{m}_i \cdot C \cdot \left(T_{r,i} - T_{s,i}\right)}{n} \qquad \text{Equation 4}$$

Values for other parameters are shown in Table 9-1.

Table 9-1. Parameter values used in calculations.

Symbol	Unit	Description	Value/Function
ε	kJ/m^3 (kWh/m^3)	The energy content of natural gas may vary. However, it was considered a constant in this study. The value used was provided by Enbridge and Union Gas and is the higher heating value (HHV).	$37{,}700$ (10.5)
C	kJ/(kg ˚C)	The specific heat capacity of glycol is not strictly a constant because it varies with the temperature[4]. The average of supply and return temperatures was used to calculate the specific heat capacity at each time step.	$C = 0.0039 \cdot T + 3.455$
ρ	kg/m^3	The flow meters used in this study provided the volumetric flow. This was converted to mass flow using the glycol density. Glycol density is not strictly a constant but varies with temperature[5]. The average of the supply and return temperatures was used to calculate the density at each time step.	$\rho = -0.0026 \cdot T^2 - 0.4407 \cdot T + 1053.9$

9.2 Cycling Derate Curve

Figure 9-1 shows capacity and efficiency over a representative cycle. It is clear that there is a ramp-up period and a steady-state period. The ramp-up period occurs from $t = 0$ to $t = t_R$ and the steady-state period occurs for $t > t_R$ until the GHP turns off. Efficiency is lower during the ramp-up period and the overall cycle efficiency is lowered when the ramp-up time comprises a notable portion of the cycle. This means that shorter cycles have a lower overall efficiency.

The impact of cycle time (t_{cyc}) on efficiency was evaluated for a number of cycles during the testing. A cycling derate was calculated for each cycle. It is shown in Equation 5 and is essentially a ratio of the overall efficiency of the entire cycle divided by the steady-state efficiency determined from $t > t_R$.

$$F_{cyc} = \frac{\eta_{overall}}{\eta_{SS}} \qquad \text{Equation 5}$$

[4] Equation determined from Fig. 15 in "A Guide to Glycol." Dow. 2003. Accessed online October 2018 at: http://msdssearch.dow.com/PublishedLiteratureDOWCOM/dh_091b/0901b8038091b508.pdf

[5] Equation determined from Fig. 16 in "A Guide to Glycol." Dow. 2003. Accessed online October 2018.

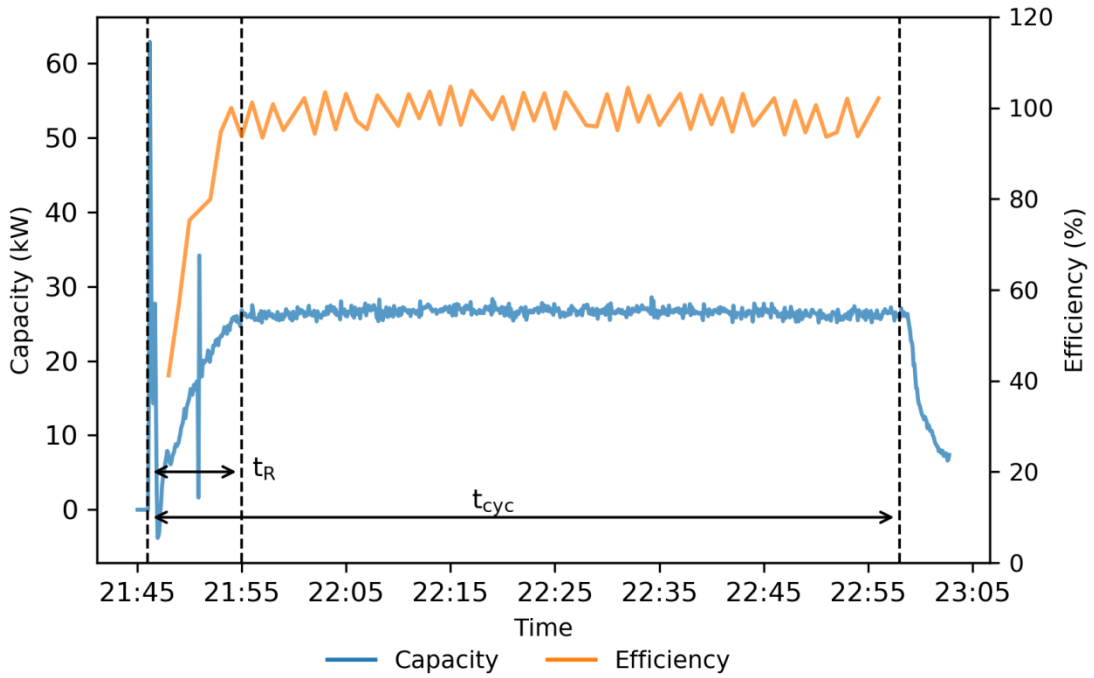

Figure 9-1. The GHP cycle goes through 2 stages: a ramp-up period and a steady-state period.

It can be shown that F_{cyc} is described analytically according to Equation 6. In fitting the experimental data, the start-up time t_R was empirically determined and α was treated as a fit parameter.

$$F_{cyc} = 1 + \frac{t_R}{t_{cyc}} \cdot \alpha \qquad \text{Equation 6}$$

9.3 Annual Heating Mode Performance Calculations

Annual performance calculations estimated the annual efficiency as well as the gas, cost and carbon savings for a variety of different scenarios considering different climates and applications. An overview of the steps used in the annual performance calculations is provided below. A sample calculation is also provided in Appendix C.

For the sake of simplicity, the cycling derate was not incorporated into the calculation. It is a dynamic parameter that is dependent upon the properties of a building and its mechanical system. The cycling derate curve can be referenced to evaluate the impact of short cycling on annual performance.

Calculation Procedure

Step 1	Select application: DHW or space-heating; boiler replacement or pre-heat system.
Step 2	Select the return temperature (32, 40 or 48 ˚C) and corresponding efficiency and capacity curves determined from a polynomial fit of the experimental performance data: $\eta(T), \dot{q}(T)$
Step 3	Define the load curve based on the application and the return temperature: $L(T)$
Step 4	Select the climate and then determine the frequency of hourly outdoor temperatures for 1 ˚C-wide bins: $n(T_i)$
Step 5	Calculate the total energy delivered to the load on an annual basis by multiplying the load for each temperature bin (in units kW) by the number of hours for that bin. $$Q_{Load} = \sum_{i=1}^{N_{bins}} L(T_i) \cdot n(T_i)$$ Equation 7
Step 6	Based on the load curve, climate, and efficiency curve, calculate the gas energy required to meet the load with the GHP. $$Q_{GAHP} = \sum_{i=1}^{N_{bins}} \frac{L(T_i) \cdot n(T_i)}{\eta(T_i)}$$ Equation 8
Step 7	Calculate the annual efficiency as a ratio of the delivered energy over the gas energy required by the GHP. $$\eta_{tot} = \frac{Q_{Load}}{Q_{GAHP}}$$ Equation 9
Step 8	Calculate the total annual operating hours of the heat pump. $$t_{Annual} = \sum_{i=1}^{N_{bins}} \left(\frac{L(T_i)}{\dot{q}(T_i)}\right) \cdot n(T_i)$$ Equation 10

Step 9

When the GHP turns on, the average electrical draw is given by $\dot{q}_{Elec}$.[6] Using the average electrical draw and the total annual operating hours, calculate the total annual electrical energy consumption.

$$Q_{Elec} = t_{Annual} \cdot \dot{q}_{Elec} \qquad \text{Equation 11}$$

Step 10

Calculate the annual energy consumption of a base case boiler.

$$Q_{Boiler} = \sum_{i=1}^{N_{bins}} \frac{L(T_i) \cdot n(T_i)}{\eta_{Boiler}} \qquad \text{Equation 12}$$

Step 11

Calculate the gas *energy* savings.

$$Q_{Savings} = Q_{GAHP} - Q_{Boiler} \qquad \text{Equation 13}$$

Step 12

Calculate the m^3 gas savings, where ε is the energy density of gas in kWh/m^3.

$$S_{Gas} = \varepsilon \cdot Q_{Savings} \qquad \text{Equation 14}$$

Step 13

Calculate the cost savings, taking account both the decreased usage of gas and the increased usage of electricity. The gas and electricity rates in units $\$/m^3$ and \$/kWh are β_{gas} and β_{Elec}, respectively.

$$S_{Cost} = \beta_{gas} \cdot S_{Gas} - \beta_{Elec} \cdot Q_{Elec} \qquad \text{Equation 15}$$

Step 14

Calculate the carbon savings resulting from the reduction in gas consumption, also taking into account the increase in electricity consumption. The electricity and gas emission factors are EF_{Gas} and EF_{Elec}, respectively.

$$S_{Carbon} = EF_{Gas} \cdot S_{Gas} - EF_{Elec} \cdot Q_{Elec} \qquad \text{Equation 16}$$

Scenarios differed based on what was selected as the load curve, climate, and return temperature. The various options that were considered are listed Table 9-2. Parameter values used in annual performance calculations are given in Table 9-3.

[6] The GHP electrical loads are primarily the pump used in the ammonia absorption cycle and the outdoor fan.

Table 9-2. Different scenarios considered in the annual performance calculations.

Load Type	Climate	Return Temperature
• Boiler replacement space heating • Boiler replacement DHW • DHW pre-heat	• Toronto • Edmonton • Vancouver	• 32 ˚C • 40 ˚C • 48 ˚C

The cost savings component of the analysis required values for the electricity and gas rates. This introduced important challenges. The first challenge was the complexity of utility rate landscape. There are various rate structures, charges, taxes, levies and other fees across the multiple jurisdictions and consumer-types applicable this study.

The second challenge is that fact that rates are not static. Any forecast of future natural gas prices will have a high degree of uncertainty and even electricity rates can deviate significantly from previously forecasted rates, as has happened recently in Ontario with the Fair Hydro Plan. The issue is further compounded by the fact that the analysis depends on the relative value of *two* rates, each with their associated uncertainties, rather than just one.

To keep the analysis simple, calculations have only been conducted using estimates of current utility rates and no fuel cost escalation has been considered. Electricity rates have been taken from a recent analysis, conducted by Hydro-Québec, of average rates for major North American cities.[7] The analysis considered different consumer classes from residential (<1,000 kWh/month) to large power consumers (>3 GWh/month). An average of the small and medium (consumption from 10,000 to 100,000 kWh/month) was used for this study.

No comparative analysis was available for natural gas rates. Estimates for these rates were generated using sample bills and rate schedules provided from Fortis, a major utility in B.C., and the Ontario Energy Board.

Note that results are also presented in terms of both m^3 gas savings and kWh electrical increases associated with GHP, as well as in terms of net cost savings. If the estimated rates considered in this study deviate significantly from future rates or particular applications, then there is sufficient information to evaluate net cost savings by looking at the projected changes in energy consumption. Note that the results of the analysis are sensitive to the utility rates estimates and a sensitivity analysis considering these parameters is recommended for prospective system owners or consultants evaluating this technology in a business case assessment.

[7] Hydro-Québec, 2018. "Comparison of Electricity Prices in Major North American Cities."

Table 9-3. Parameter values used for the annual performance calculations.

Symbol	Parameter Description	Value
η_{Boiler}	This is the base case efficiency assumed for a boiler. The value was provided by TAF and is intended to represent an annualized efficiency including real-world losses, similar to an AFUE.	0.88
$\beta_{gas,Toronto}$	This is the unit cost of gas for Toronto. It was estimated using the Ontario Energy Board bill calculator for small commercial applications and includes all relevant fees and charges (delivery, gas supply charge, cost adjustment, transportation charges, and HST) neglecting fixed customer charges.	0.30 $/m^3$
$\beta_{elec,Toronto}$	This is the unit cost of electricity for Toronto. It was estimated using the analysis from Hydro-Québec.	0.14 $/kWh
$\beta_{gas,Vancouver}$	This is the unit cost of gas for Vancouver. It was estimated using sample bills and rate schedules from FortisBC for small commercial applications. It includes all relevant fees and charges (delivery, storage and transport, cost of gas, GST, carbon tax, clean energy levy and municipal operating fee) neglecting fixed customer charges.	0.33 $/m^3
$\beta_{elec,Vancouver}$	This is the unit cost of electricity for Vancouver. It was estimated using the analysis from Hydro-Québec.	0.12 $/kWh
$\beta_{gas,Edmonton}$	This is the unit cost of gas for Edmonton. It was estimated as the average of the rates for Toronto and Vancouver, because available resources were less clear on how to select an appropriate rate.	0.32 $/m^3
$\beta_{elec,Edmonton}$	This is the unit cost of electricity for Edmonton. It was estimated using the analysis from Hydro-Québec.	0.15 $/kWh
EF_{Gas}	This is the emission factor for the combustion of natural gas. It was obtained from the National Inventory Report.	1.89[8] kg CO_2e/m^3
$EF_{Elec,Toronto}$	This is the emission factor for electricity in Toronto. The value was provided by TAF and is a result of their own analysis of marginal electricity emission factors.	0.159[9] kg CO_2e/kWh
$EF_{Elec,Edmonton}$	This is the emission factor for electricity in Edmonton. A marginal emission factor was not available. This annualized emission factor includes losses from transmission and distribution and was taken from the 2018 National Inventory Report (Table A13-10).	0.900 kg CO_2e/kWh
$EF_{Elec,Vancouver}$	This is the emission factor for electricity in Vancouver. A marginal emission factor was not available. This annualized emission factor includes losses from transmission and distribution and was taken from the 2018 National Inventory Report (Table A13-11).	0.012kg CO_2e/kWh

[8] Environment Canada. 2013. National Inventory Report 1990-2011 (Part 2-A8): Greenhouse Gas Sources and Sinks in Canada.

[9] TAF. 2017. "A clearer view on Ontario's emissions: Practice guidelines for electricity emissions factors." Table 1.

9.3.1 Climate

Weather data files from the CWEC database for each city were aggregated according to the number of hours that the ambient outdoor temperature occurred within defined 1 ˚C wide temperature bins. Within the calculation procedure, the number of hours that the outdoor temperature fell into a given temperature bin is denoted by $n(T_i)$ where T_i is the mid-point of the bin. As an example, $n(2.5)$ represents the number of hours in a given climate where the outdoor temperature fell between 2.0 and 3.0 ˚C. The hourly distribution of outdoor temperatures for different locations is shown in Figure 9-2.

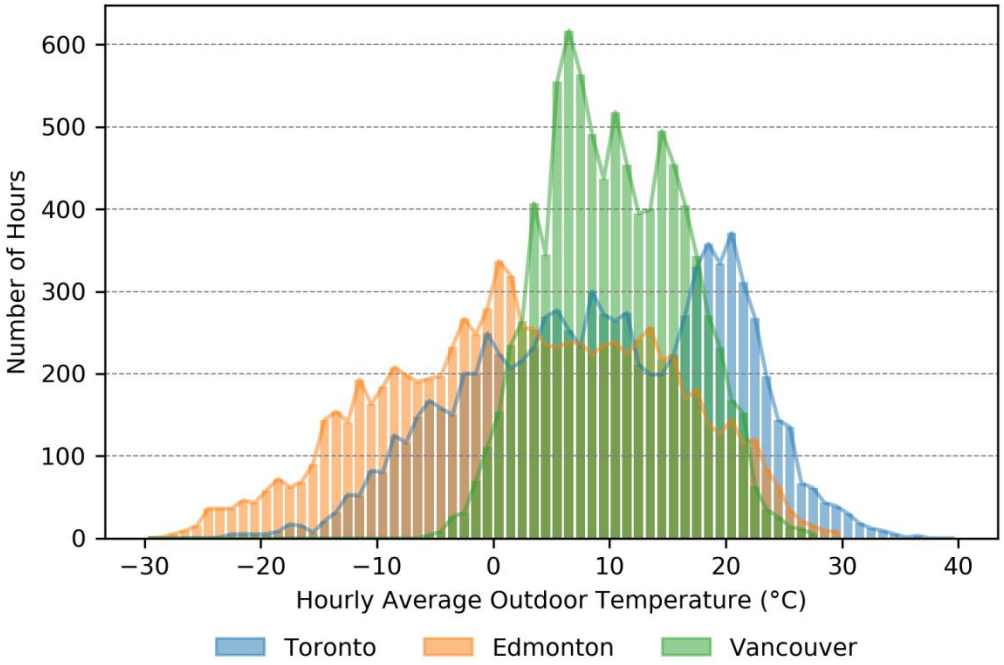

Figure 9-2. The hourly distribution of temperatures for each location considered.

9.3.2 Return Temperature

Based on the performance map data, polynomial fits of the capacity and efficiency curves were calculated for each return temperature and the fit equations were used in annual performance calculations. Not all return temperatures were considered for each load type. For example, DHW boiler replacement applications only considered the 48 ˚C return temperature and DHW pre-heat applications only considered the 32 ˚C return temperature.

9.3.3 Load Type

Boiler replacement space heating

Representative linear building load curves were created to match the GHP capacity curves. The building load curves were defined such that there was zero load at an assumed building balance point

of 18 ˚C and the building load was equivalent to the corresponding GHP capacity at the design temperature for that climate (Figure 9-3).

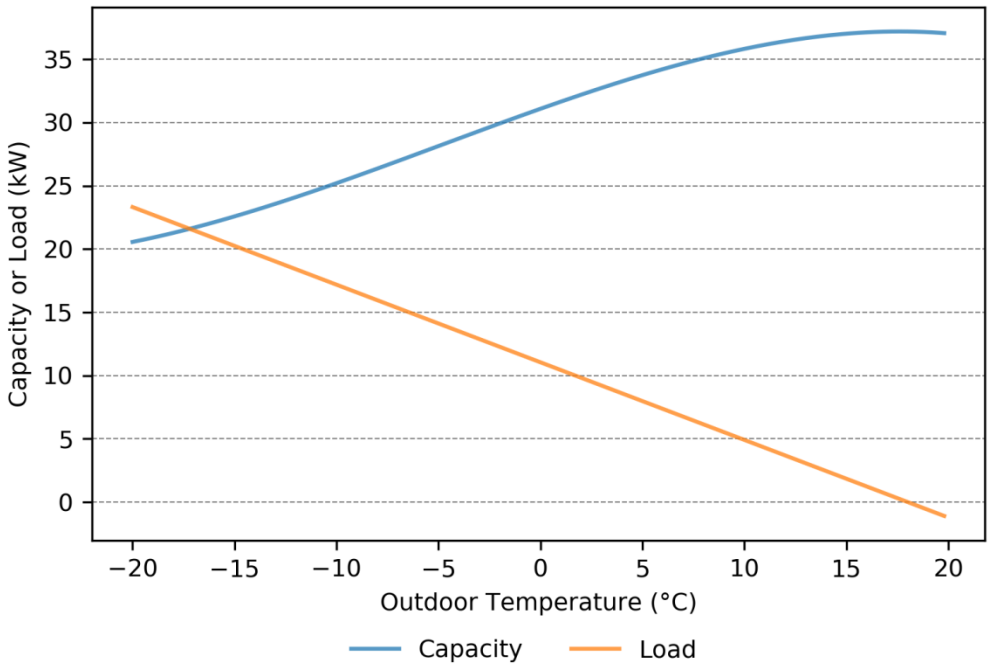

Figure 9-3. Example space heating load curve for a boiler replacement, assuming a Toronto location and a 32 ˚C return.

Boiler replacement DHW

As with space heating, a representative DHW load was assumed so as to perform the calculation. The calculation made the following assumptions:

1. the DHW load is constant,
2. under the design outdoor temperature, the GHP is sufficient to meet the load,
3. the curve that closest approximates a DHW load is that for a return of 48 ˚C (and a supply of 58 ˚C) and the corresponding capacity and efficiency curves were used in the analysis.

An example load and capacity curve is shown in Figure 9-4.

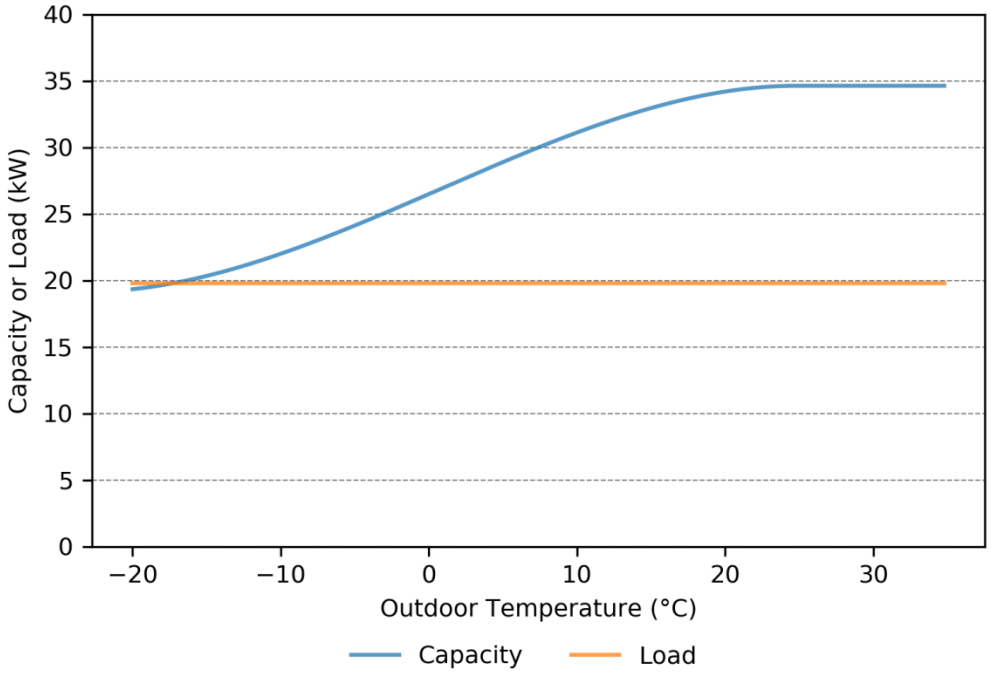

Figure 9-4. Example DHW load curve for a boiler replacement. It is equivalent to the GHP heating capacity at the design conditions for a given climate.

DHW Pre-heat

This option only considered a DHW application, without space heating. Calculations assumed that the overall load was large enough that the GHP could be operated at full capacity all the time in a pre-heat capacity utilizing a low return temperature (32 ˚C). See Figure 9-5.

Load Summary

It is clear that the different load profiles represent different degrees of heat pump utilization. In the space heating scenario, the load is only present when the outdoor temperature is below a certain value. It is also the case the unit has more capacity than needed for most outdoor temperatures and will need to cycle off to prevent overheating. In the context of the annual performance calculations, this reduced the operating hours and overall gas savings.

The DHW boiler replacement scenario assumed the unit is present round and this increases operating hours. However, the unit would still be oversized and need to cycle off for warmer temperatures. The DHW pre-heat scenario assumed the unit is perfectly matched to the load and will be able to operate all the time. This would promote the greatest savings because the heat pump would be utilized to the greatest degree.

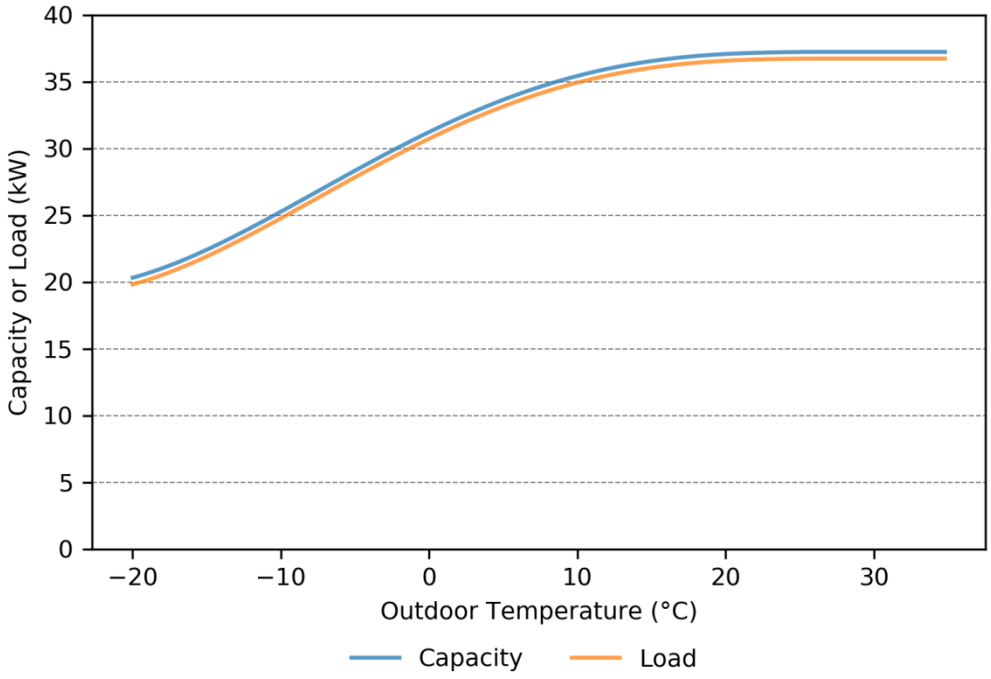

Figure 9-5. Example pre-heat system load curve. This scenario assumes that the GHP can run all the time and utilize a low return temperature.

9.4 Annual Cooling Mode Performance Calculations

High level carbon and cost calculations in *cooling mode* were performed and are summarized in Section 10.5 They are presented as worked examples and a detailed description is not provided here.

9.5 Analysis Summary

Using the capacity and efficiency data collected during steady-state testing, the GHP annual efficiency was evaluated within an hourly bin analysis for different scenarios, including different locations and applications.

Assumptions about building loads were required to perform the analysis. These assumptions were made to be as simple as possible while still sufficiently capturing the impacts of the factors considered. Space heating loads were assumed to be a linear with ambient temperature. They matched the heating system capacity at the design temperature corresponding to the given climates and were zero at an assumed building balance temperature of 18 ˚C. Domestic hot water loads were assumed to be constant with ambient temperature for the boiler replacement scenario and equivalent to the GHP capacity at all ambient temperatures for the DHW pre-heat scenario.

In general, the aim of the analysis was to appropriately weight or derate the GHP performance curves according to location and application; to identify a range of expected efficiencies and savings potentials. Assumptions made within the analysis were sufficient for this purpose. The authors

acknowledge that more rigorous building energy modelling would be required to estimate the GHP performance for specific buildings.

10.0 RESULTS & DISCUSSION

10.1 Heating Mode Steady-state Performance map

In total, 57 heating mode tests were performed to determine the steady-state performance of the GHP. Steady-state capacity curves are shown in Figure 10-1. Efficiency results (according to HHV) are shown in Figure 10-2. Efficiency results only take into account gas consumptions. Electricity consumption was considered separately. Outdoor temperatures from -27 ˚C to 32 ˚C were observed with sufficiently complete datasets for each return temperature considered. Three different pump settings were explored with flow rates ranging from 10 to 16 gpm but flow rate did not have a discernable impact on performance and it is not considered in the figures.

Note that there was insufficient data at the endpoints of the curves to ensure an accurate fit in those regions and fit curves were forced to a constant value. Also, note that these curves reflect the use of a 50% propylene glycol heat transfer fluid rather than water. This is necessary in a cold climate. However, since glycol has poorer heat transfer properties, it degrades the GHP capacity and efficiency. A discussion of this is provided in Appendix A. Ultimately, there is not enough data available to determine how 50% glycol affected the capacity and efficiency across the range of outdoor temperatures and return temperatures considered.

The manufacturer reported efficiency is also plotted. The manufacturer data point was determined with water as a heat transfer fluid rather than 50% propylene glycol, and with a return temperature of 40 ˚C. The manufacturer data point is 8 % (percentage points) above the corresponding experimental value determined in this study (the orange curve). Given that some amount of degradation is expected due to the glycol heat transfer fluid, there appears to be reasonable agreement between the manufacturer data and the experimental data collected in this study.

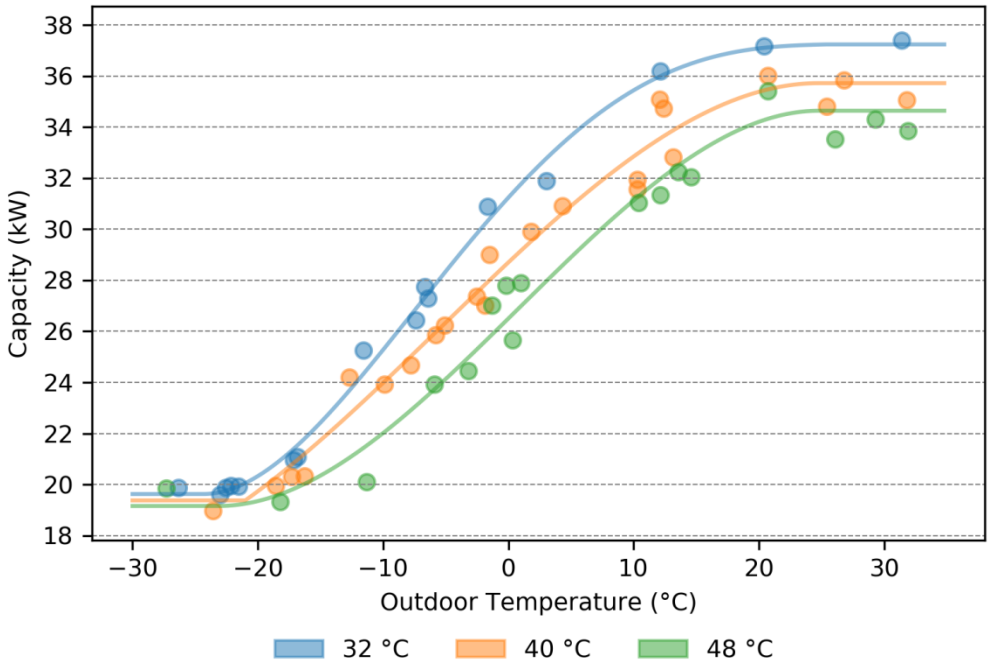

Figure 10-1. Steady-state capacity of the GHP for different return temperatures.

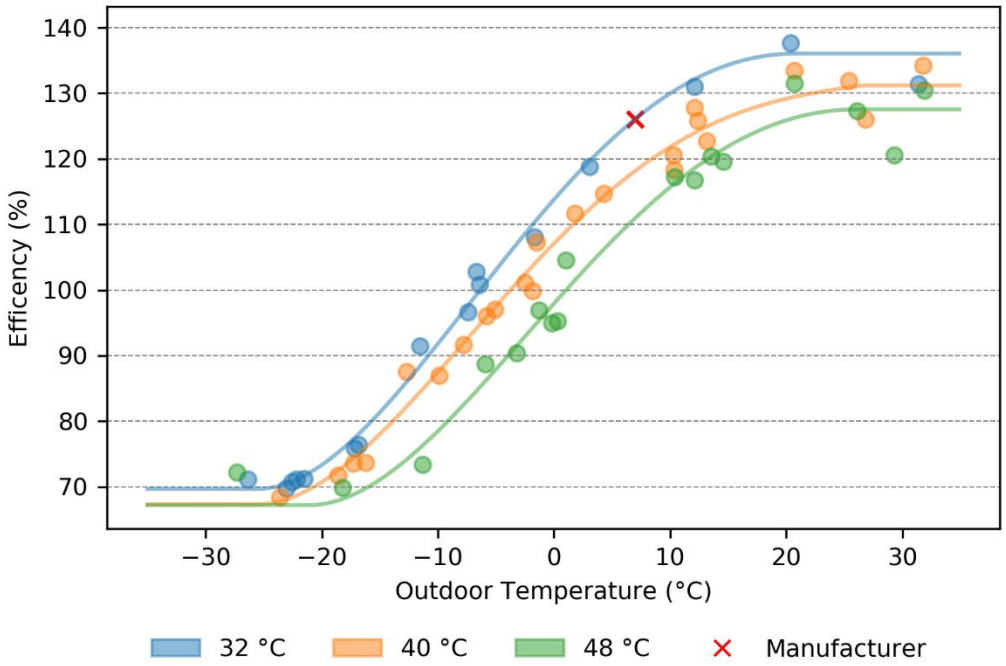

Figure 10-2. Steady-state efficiency curves of the GHP (according to gas HHV).

10.2 Annual Efficiency

The calculated annual efficiencies for space heating and DHW are shown in Figure 10-3. The first label "DHW-PH" indicates a DHW pre-heat application. The second label "DHW" indicates a replacement for a boiler in a DHW application. The other labels indicate space heating applications with a return temperature of either 32 ˚C, 40 ˚C or 48 ˚C. These applications are described in Section 9.3.3

The DHW-PH scenario is most efficient because it has lower return temperatures and more operating hours at higher efficiency operating points (when ambient temperatures are warm) and this pulls the weighted annual efficiency to a greater value. Note that the efficiency given in Figure 10-3 is the annual efficiency of the GHP *only* and not that of an entire gas heat pump and boiler hybrid system.

The greatest space-heating efficiency was for low-temperature heating in Vancouver. This is because both low return temperatures and warm ambient outdoor temperatures promote greater efficiency. It is important to note that Vancouver would not require a 50% propylene glycol and the annual efficiency would be even higher than reported here. However, there is not enough to data to know precisely how much higher. Appendix D considers different scenarios and the impact on the savings in Vancouver.

The lowest efficiency option was high-temperature space heating in Edmonton. In fact, due to the cold outdoor ambient temperatures and high-return temperatures, this scenario was estimated to have a *lower* efficiency than that of a high-efficiency boiler. This immediately demonstrates that, while high efficiencies are achievable in some scenarios, a gas heat pump is not an effective solution for *every* application and *every* climate.

The relative gas savings as a function of the annual GHP efficiency, as compared to a high-efficiency boiler, is shown in Figure 10-4. A 124% annual efficiency (DHW-PH in Toronto or SH-32 in Vancouver) translates to a relative gas savings of roughly 30%. A 109% annual efficiency (SH-32 in Toronto) translates to gas savings near 20%. Recall that the base case boiler efficiency was assumed to be 88% efficient. This number was suggested by TAF and is intended to represent an as-installed annualized boiler efficiency incorporating real-world losses.

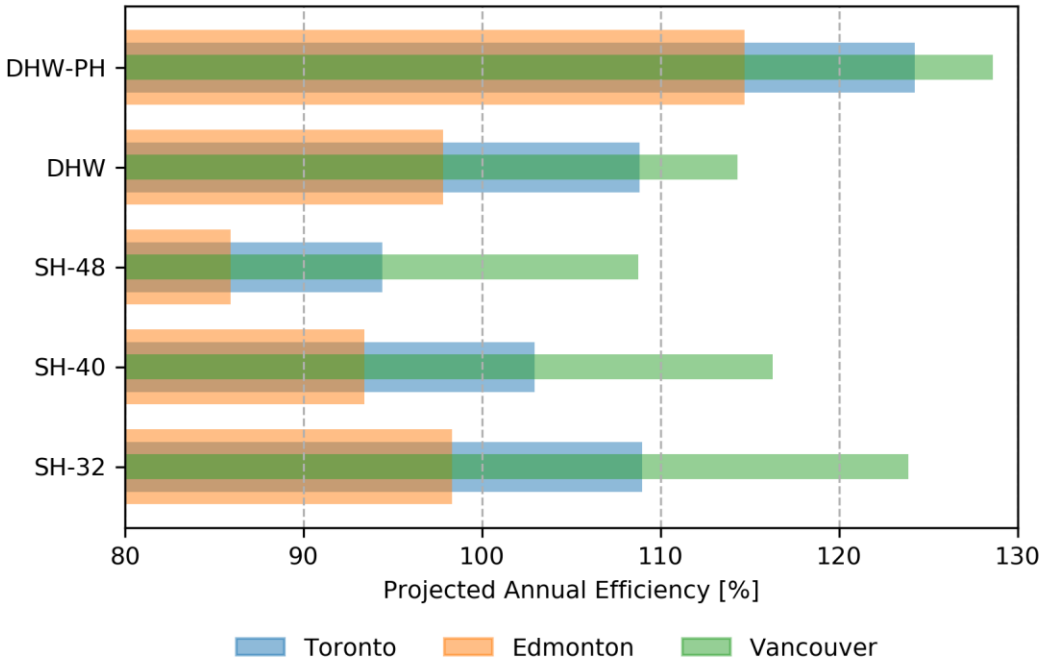

Figure 10-3. Projected annual GHP heating efficiency for different scenarios.

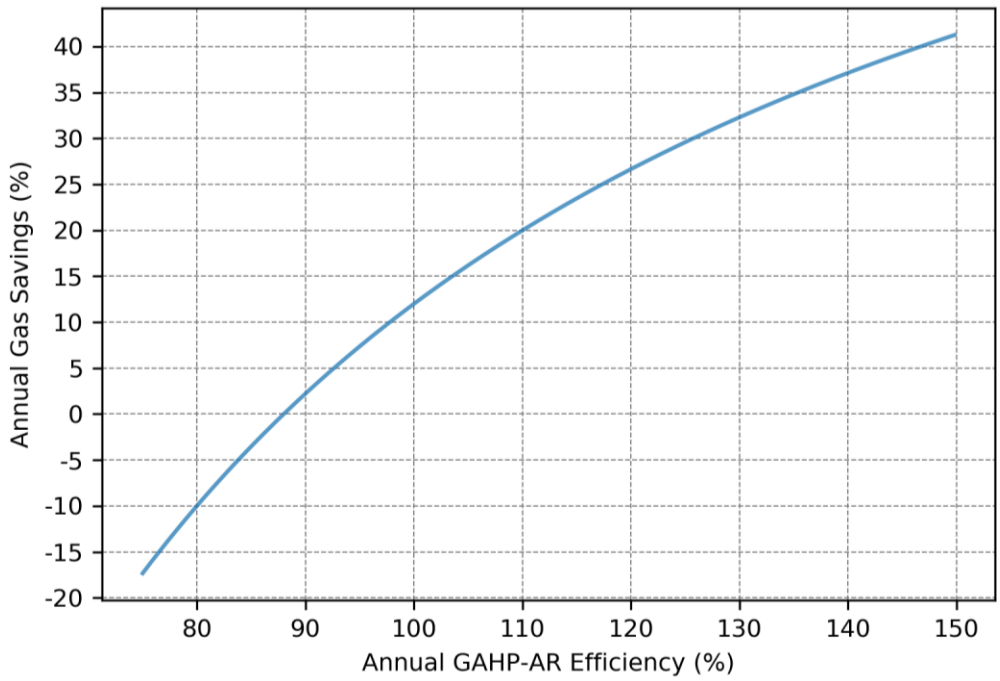

Figure 10-4. The annual heating efficiency of the GHP determines the relative gas savings.

10.3 Savings

Projected annual gas savings are plotted in Figure 10-5. Gas savings varies greatly across the scenarios considered. There is greater savings in warmer climates because efficiency improves with higher outdoor ambient temperatures. DHW applications have greater savings because there are more operating hours and warmer outdoor temperatures. Operating hours are shown in Figure 10-6 for Toronto. DHW pre-heat applications have even greater savings than DHW boiler replacement applications because, in addition to more operating hours and warmer ambient temperatures, DHW pre-heat applications have a low-return temperature and therefore a greater efficiency.

Annual electricity consumption is shown in Figure 10-7. Electricity consumption was measured in this study and determined to be a constant 1.06 kW load whenever the GHP was on in a steady-state, regardless of the outdoor ambient temperature. The European specifications claim a nominal operating power of 0.9 or 0.93 kW depending on whether a low-noise fan is selected and the North American specifications claim a nominal operating power of 0.75 kW. The power measured in this study is therefore near the European nominal rating but notably larger than that for North American. The reason for the discrepancy between the European and North American specifications, and the somewhat higher power measured in this study, are not clear.

Net cost calculations considered the increase in electricity consumption against the decrease in natural gas consumption. Figure 10-8, showing annual net cost savings, summarizes one of the most notable findings of the study – DHW pre-heat applications are anticipated to have a very large annual net cost savings and savings is lower for all other applications. Even DHW boiler replacement applications, which would seem quite similar to pre-heat applications at first glance, are estimated to have a notably lower net cost savings. The key issue is that the GHP is not just a gas heating appliance. It consumes both gas *and* electricity. Gas savings are obtained at the expense of electricity consumption, and the gas savings need to be much greater than the electricity consumption to have an overall net cost savings. This is further illustrated in Figure 10-9.

Figure 10-9 breaks down the annual cost savings for the two DHW scenarios, pre-heat and boiler replacement, according to outdoor ambient temperatures. Summing all the bars shown in this plot would produce the total annual net cost savings. The temperature at which the GHP efficiency, and resulting gas savings, are great enough to offset the additional electricity consumption is the point where the net cost savings goes from negative to positive.

This break-even point is important because every temperature below it generates a cost and every temperature above it, a savings. The total savings needs to be greater than the total cost in order to result in net savings. It is clear from the figure that the high-return temperature (and lower efficiency) is hindering the DHW boiler replacement application because it pushes this break-even point to warmer temperatures, increasing costs and reducing savings. The reason for the disparity between the DHW boiler replacement and pre-heating scenarios shown in Figure 10-8 is then clear. Operating hours are greater for DHW pre-heating but more importantly, the lower return temperature, and

therefore higher efficiency, pushes the break-even point to colder temperatures. This promotes savings and reduces costs.

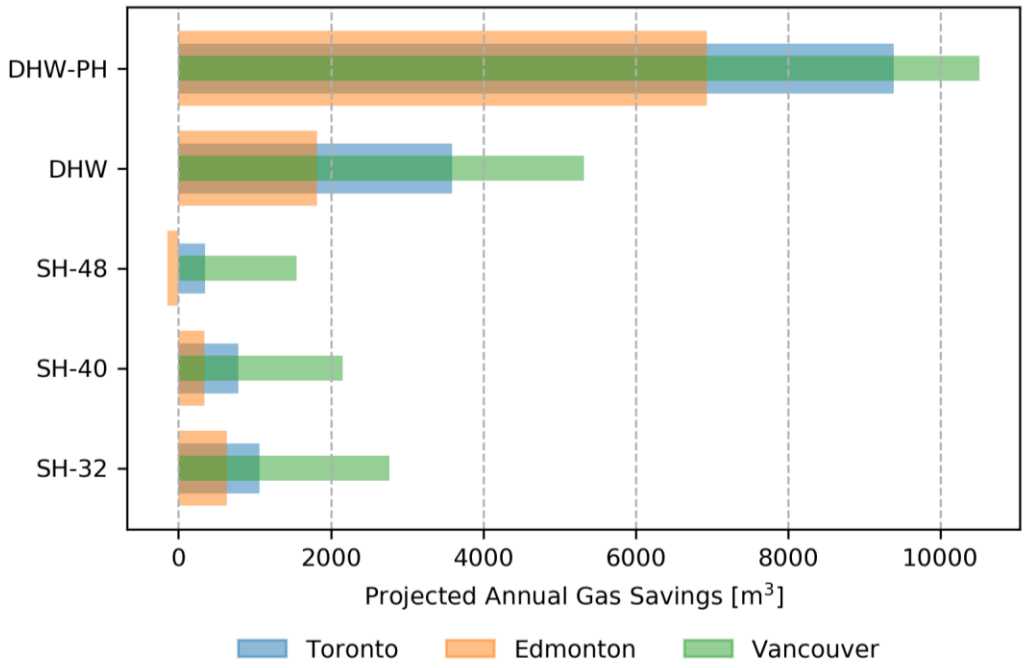

Figure 10-5. Projected annual gas savings of the GHP.

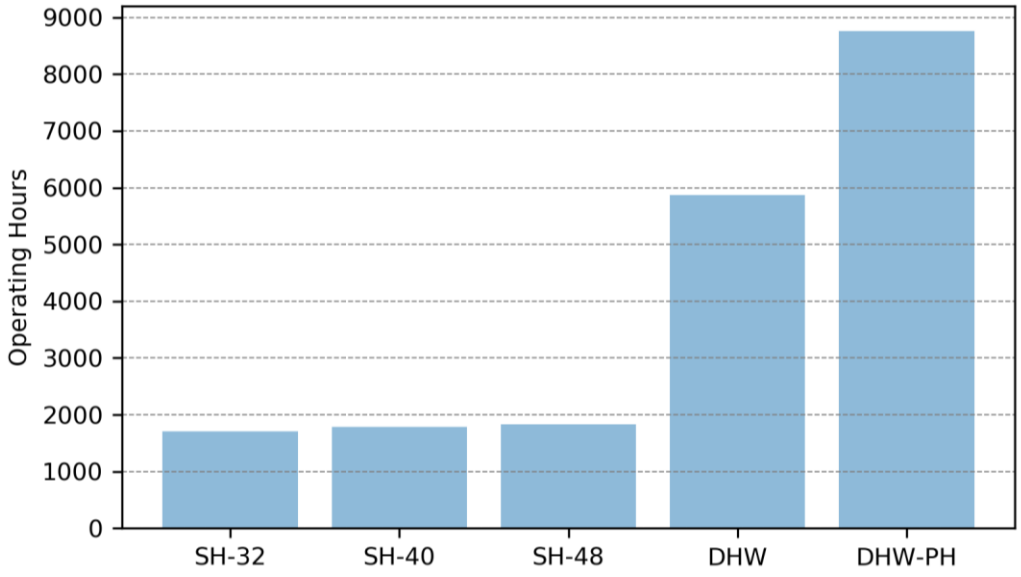

Figure 10-6. The GHP operating hours for Toronto are greatest for DHW applications.

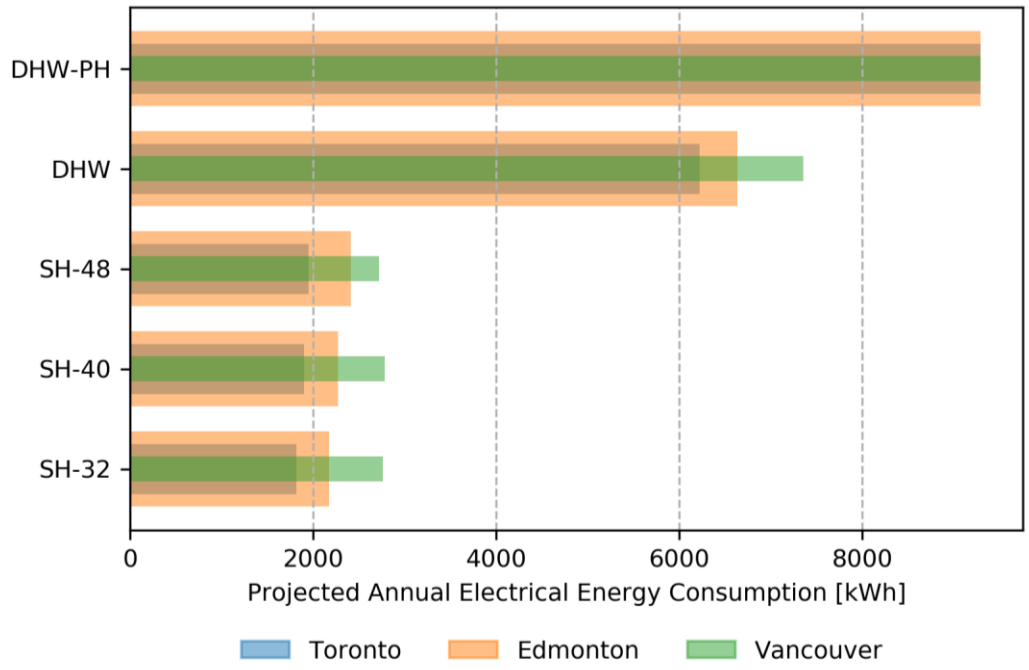

Figure 10-7. Projected annual electricity consumption of the GHP. Electricity consumption in Vancouver is greater because the warmer Vancouver design temperature means the GHP capacity curve is closer to the load curve for all operating points. This means it cycles less and operates for a greater number of hours.

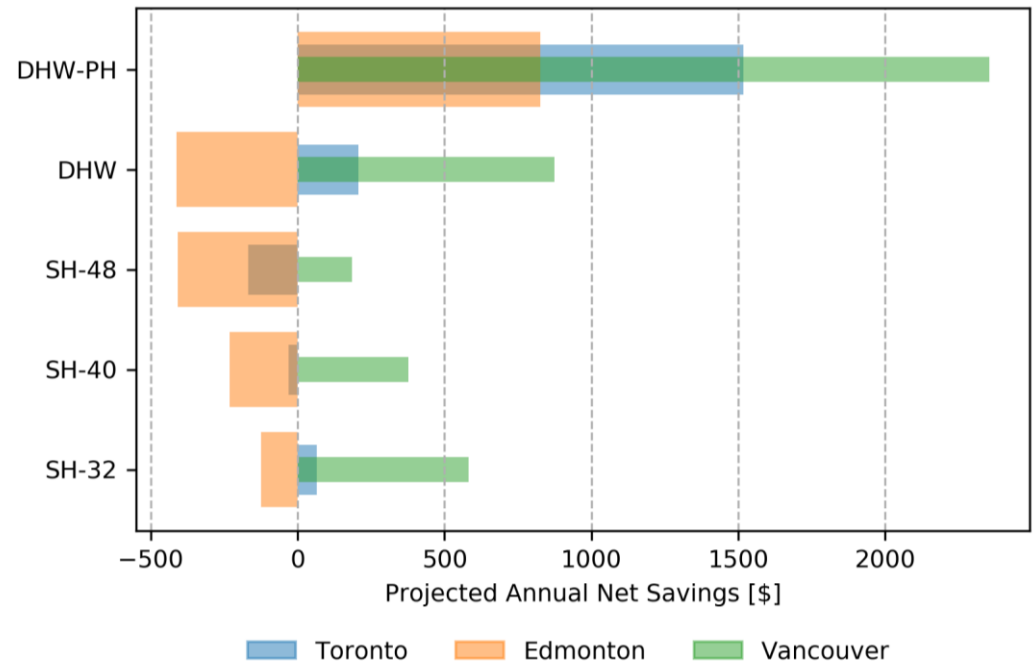

Figure 10-8. Annual cost savings projections take into account both the gas savings and the increase in electricity consumption but not incentives, rebates or carbon pricing. Annual net savings is greatest for DHW-PH, in part, because this application's higher efficiency means more gas is being saved for every kWh consumed.

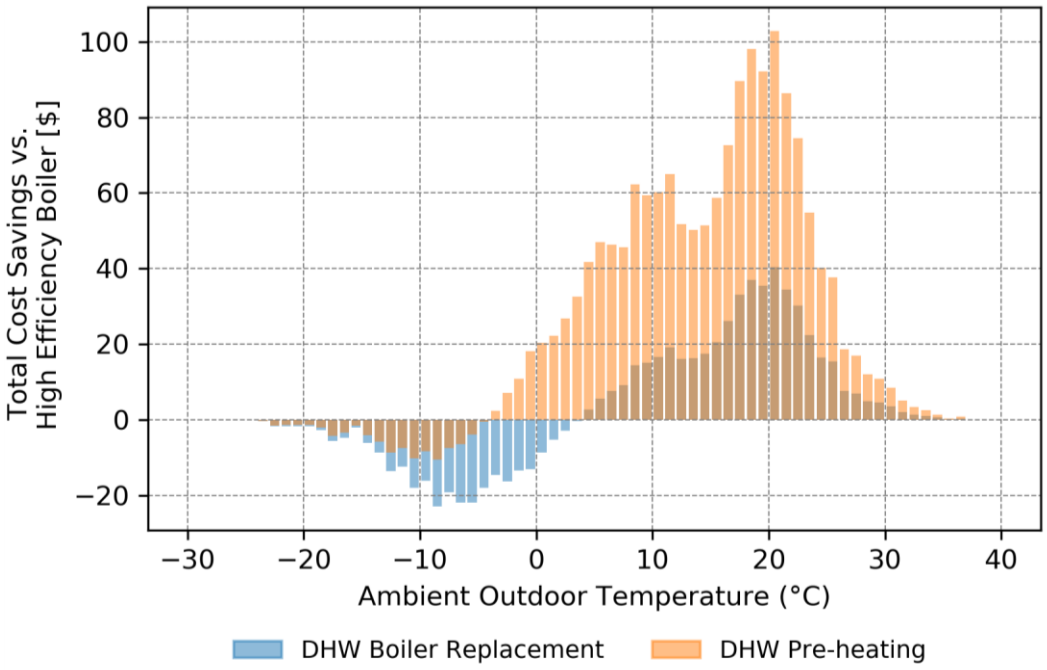

Figure 10-9. The GHP actually results in a net increase in cost for lower temperatures when compared to a high-efficiency boiler. This is because the gas savings is lower than the cost of additional electricity consumption. For lower return temperatures, as in DHW pre-heating, the break-even point occurs at lower ambient outdoor temperatures and there are fewer hours where the GHP operates at a loss with respect to cost.

This phenomena also explains why some of the higher-temperature space-heating scenarios did not result in savings (as shown in Figure 10-8); efficiencies were not high enough such that the gas savings could offset the cost of additional electricity consumption.

The additional electricity cost is substantial. As an example, in the DHW-PH application in Toronto, the GHP was calculated to save 9,391 m^3 of gas per year with an estimated associated value of $2,817. However, to do that, it needed to operate for 8760 hours while consuming 1.06 kW of electricity. This resulted in 9,286 kWh of electricity consumption with an estimated associated cost of $1,300. The net cost savings is then $1,517 and it is clear that electricity consumption significantly impacts the net savings.

The net cost savings calculations did not take into account rebates, incentives or carbon pricing. However, it is clear from Figure 10-10 that carbon savings are substantial for some applications and, if the GHP could benefit from a carbon pricing program, it could further improve the business case quite significantly. For example, a carbon price of 50$ per ton would add another $813 per year onto the annual net savings of DHW pre-heat application in Toronto – bringing the total net savings to closer to $2,300 per year.

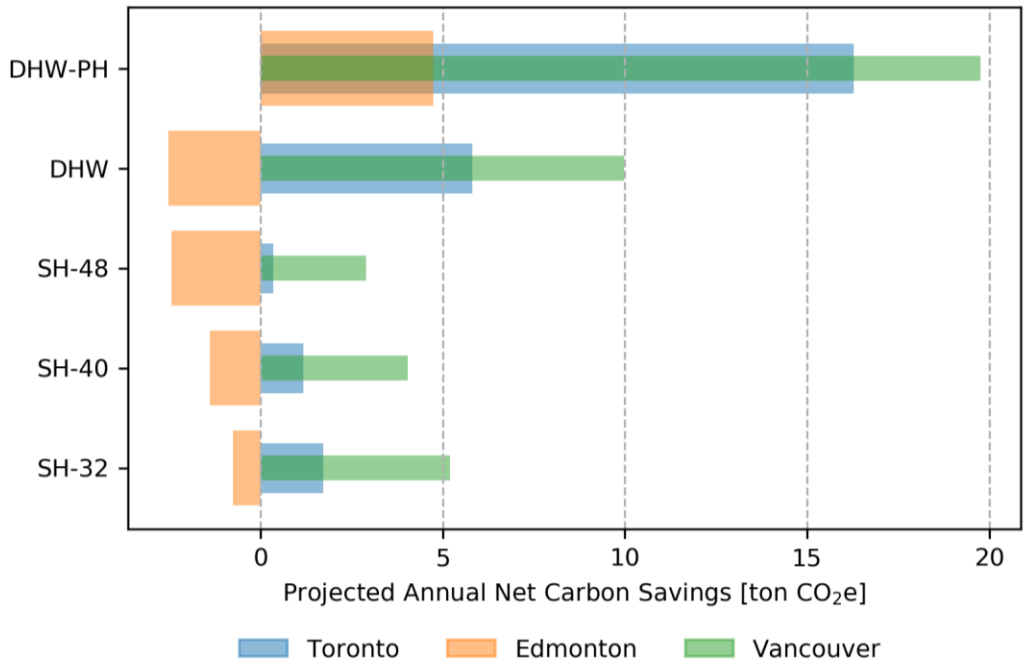

Figure 10-10. The annual carbon savings calculations took into account both the gas savings and the electricity increase. Carbon *increases* are seen for Edmonton because of the high electricity grid emission factor and lower efficiency in this climate.

10.4 Cycling Testing

Cycling testing was done throughout the heating mode monitoring period. The GHP was simply allowed to cycle normally to meet the load of the ASH. Set-point parameters were configured to encourage cycles of different length. Individual cycles were then extracted from the data trends and analyzed to determine the cycling factor. There was no significant correlation observed between the cycling factor and any other parameters aside from the cycle time (i.e. cycling derate factor was not affected by outdoor temperature, return temperature, etc.).

Individual cycling factor data points were determined from individual cycles and fit to the analytical equation shown in Equation 6 where $t_R = 8.14$ and α was determined as a fitting parameter. Results from 36 different cycles are shown in Figure 10-11. It is clear that the cycle time has a notable impact on the overall efficiency. For example, at 15 minutes, the cycling derate factor is 0.78. This means the actual efficiency for a 15 minute cycle is 22% lower than the steady-state efficiency. Beyond 35 minutes the cycle factor is greater than 0.90 and beyond 70 minutes, it's greater than 0.95. To achieve optimal efficiency in practice, longer cycle times should be encouraged within the system design and control.

$$F_{cyc}(t_{cyc}) = 1 - \frac{3.35}{t_{cyc}} \qquad \text{Equation 17}$$

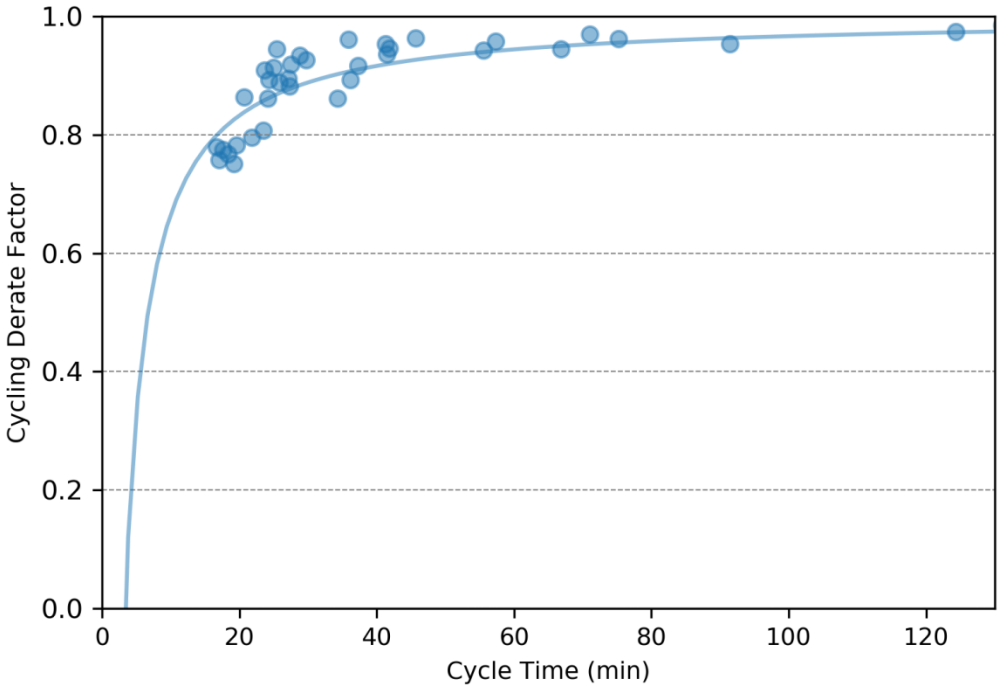

Figure 10-11. Overall efficiency is lower for shorter cycles due to start-up losses.

A detailed description of techniques to promote long cycle times for different applications is beyond the scope of this report. However, a few considerations are discussed here in brief. Thermostats and aquastats have deadbands as well as set-points. A deadband is necessary to prevent rapid on/off calls to the heating equipment. For example, a thermostat with a 1 °C deadband and a 22 °C set-point would cause the heating to turn on at 21.5 °C and off at 22.5 °C. Larger deadbands mean longer cycles but larger dead bands on a room thermostat impact the thermal comfort of occupants because they result in greater temperature fluctuations. This may be mitigated though the use of a buffer tank.

In a system with a buffer tank, the heat pump would provide heat *to* the tank and the load would pull heat *from* the tank. The buffer tank effectively decouples the load from the GHP. The co-ordination of the heat provided to the load from the tank would be controlled by room thermostats but the heat pump would be controlled by an aquastat on the buffer tank. The aquastat would tell the heat pump to turn on when the tank dropped below a certain temperature and off when the tank reached a certain temperature. A larger tank would take longer to heat up and, if the load is simultaneously pulling heat from the tank, then the heat pump cycle time would be even longer.

It follows that the heat pump cycle time would depend on at least three things: the buffer tank size, the aquastat deadband and the nature of the load. In optimizing the cycle time, designers would need to consider these factors among many others, such as: the additional cost associated with a larger buffer tank against the benefits it provides, how to interface the GHP with the tank, cost optimization of heat exchanger sizing (if a heat exchanger is used), as well as other factors. In larger buildings, it may also be possible to promote longer cycle times using a building automation system (BAS) or other building control approaches.

10.5 Cooling Mode Steady-State Capacity and Efficiency

The performance map of cooling capacity and efficiency are shown in Figure 10-12 and Figure 10-13. Both show that there is a slight decrease in performance as outdoor temperatures increases. Any impacts related to flow rate or return temperature were not discernable from the dataset.

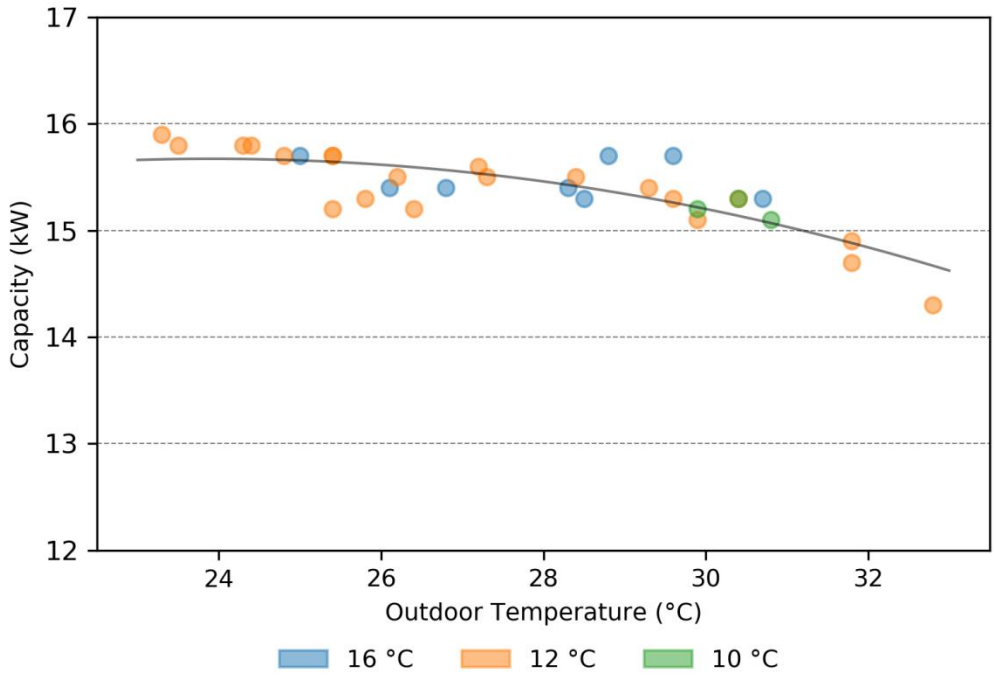

Figure 10-12. Capacity decreases slightly with increasing outdoor temperature.

Considering only gas consumption, the cooling mode efficiency is approximately 57% for the majority of relevant temperatures. In other words, the heat pump removes 0.57 units of heat energy for every 1 unit of gas energy it consumes. In contrast, a high-efficiency electric air-conditioner may have an energy efficiency ratio (EER) of 14, which equates to 4.1 units of heat energy removed for every 1 unit of electrical energy it consumes. It follows that, for the same *energy* input, the electric air conditioner removes 7.2 times more heat energy. The impact of the low efficiency on utility costs is explored in Example 1 using Ontario residential utility rates (October 2018).

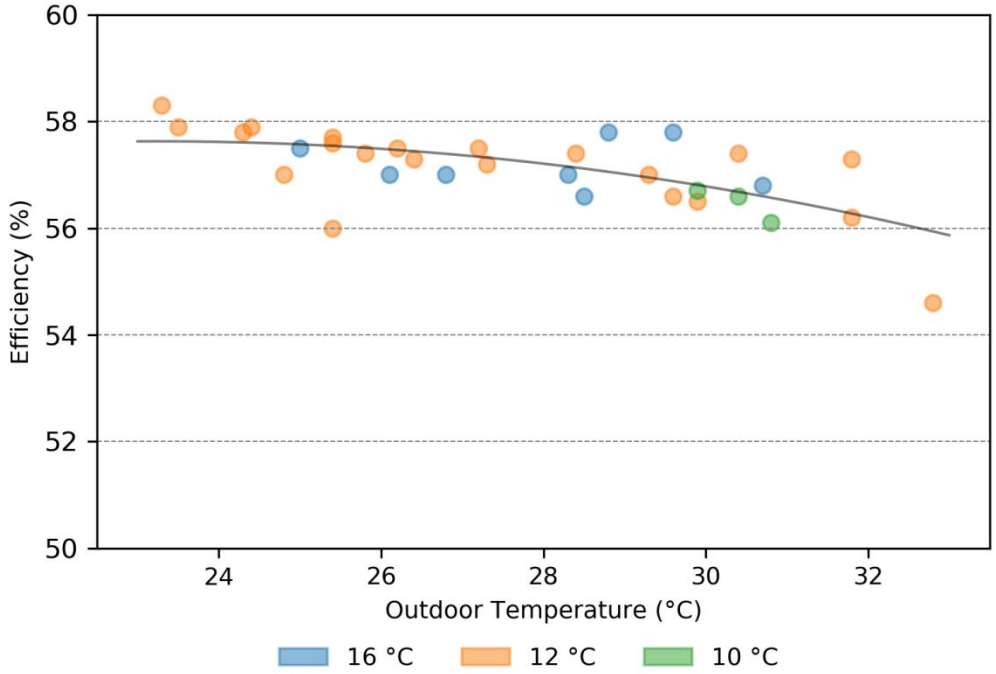

Figure 10-13. Efficiency decreases slightly with increasing outdoor temperature.

Example 1: *Cost of cooling with gas versus cooling with electricity*

Assume the following:

- *peak, mid-peak and off-peak rates for electricity are 0.19, 0.15 and 0.12 $/kWh, respectively, taking into account all applicable taxes and charges,*
- *gas rate is 0.30 $/m³,*
- *gas energy density is 37,700 kJ/m³ (10.5 kWh/m³),*
- *gas cooling efficiency is 57%, and*
- *electric air-conditioner EER is 14 (equivalent to 410% efficient).*

The cost to remove 1 kWh (thermal)[10] of heat energy using gas is 0.050 $.

$$1kWh \cdot \left(\frac{1}{0.57}\right) \cdot \left(\frac{m^3}{10.5\ kWh}\right) \cdot \left(\frac{0.30\ \$}{m^3}\right) = 0.050\ \$$$

[10] Note that a kWh is a unit of energy, just like a GJ or Btu. It is used as a unit of heat energy in these examples to avoid unnecessary conversion back-and-forth between different units. The context should make it clear whether the calculations is referring to a thermal kWh or an electrical kWh.

The cost to remove 1 kWh of heat energy using peak electricity is 0.046 $.

$$1kWh \cdot \left(\frac{1}{4.1}\right) \cdot \left(\frac{0.19\ \$}{kWh}\right) = 0.046\ \$$$

The cost to remove 1 kWh of heat energy using off-peak electricity is 0.029 $.

$$1kWh \cdot \left(\frac{1}{4.1}\right) \cdot \left(\frac{0.12\ \$}{kWh}\right) = 0.029\ \$$$

It follows that the energy cost of cooling with gas during any time-of-use bracket is more expensive than electrically-driven cooling. This is without even considering the electrical consumption of the GHP. Per kWh electricity rates may be lower for commercial or industrial applications and this would worsen the results for the GHP.

It could also be argued that a benefit of the GHP is the reduction peak demand charges. In that scenario, it would be worthwhile to evaluate the kW demand of electricity for every kW of heat removed for the GHP versus that for electric cooling.

Note the following:

- *The electrical demand of the GHP is 1 kW.*
- *The max cooling capacity is ~15.5 kW.*
- *Assumed electric air-conditioner EER is 14 (equivalent to 410% efficient).*

The electrical demand to remove 15.5 kW of heat energy with an electric air-conditioner is 3.8 kW. It follows that electrically-driven cooling requires approximately 4 times greater electrical demand to remove an equivalent amount of heat when compared with the GHP.

$$15.5\ kW \cdot \left(\frac{1}{4.1}\right) = 3.8\ kW$$

In summary, utility costs associated with per unit usage of gas and electricity would increase with the use of a GHP but electrical demand charges (if applicable) would decrease. The relative impacts of these two factors would require a deeper analysis of rate structures for the jurisdictions considered, as well as analysis of different building types and demand profiles. This is beyond the scope of this study. It is clear that utility costs would increase for smaller consumers (that don't pay electrical demand charges) but, for larger consumers, it is feasible that reduced electrical demand charges could offset or possibly negate those increases. It was not determined whether the balance would lie at a net cost or a net savings (for larger consumers) due to the complexity of the analysis and the various factors that need to be considered.

The difference in cooling mode efficiency also has important implications for carbon emissions. The GHP requires much more energy to provide the same level of cooling when compared to an electric alternative. Furthermore, that energy comes in form of the direct combustion of natural gas, which has a high emission factor. The most optimistic scenario for the GHP might assume that the direct combustion of gas for cooling via a gas heat pump would offset natural gas that is used in the electricity grid – and that direct combustion may be a better option than transforming that gas energy into electricity and then transporting it through the electricity grid with its associated losses. This is evaluated in Example 2, below. Again, assumptions are based around an Ontario jurisdiction but they do not deviate significantly for the other jurisdictions considered within this study.

Example 2: *Carbon emissions of cooling with gas versus cooling with electricity*

Assume the following:

- *the EF for combustion of natural gas is 1890 g CO_2e/m^3;*
- *the energy density of gas is 10.5 kWh/m^3;*
- *the EF of the gas-powered electricity generation is 400 g CO_2e/kWh*[11].

Using these values, the EF of gas combustion per unit energy can be calculated as 180 g CO_2e/kWh.

$$\left(\frac{1890\ g\ eCO_2}{m^3}\right)\cdot\left(\frac{m^3}{10.5\ kWh}\right)=180\ \frac{g\ CO_2e}{kWh}$$

Taking into account efficiency, the emissions resulting from the removal of 1 kWh of heat energy with the gas heat pump is:

$$1\ kWh\ \cdot\left(\frac{180\ g\ eCO_2}{kWh}\right)\cdot\left(\frac{1}{0.57}\right)=316\ g\ CO_2e$$

The emissions resulting from the removal of 1 kWh of heat energy with an electric air conditioner:

$$1\ kWh\ \cdot\left(\frac{400\ g\ eCO_2}{kWh}\right)\cdot\left(\frac{1}{4.1}\right)=98\ g\ CO_2e$$

[11] The National Renewable Energy Laboratory (NREL) in the U.S. has evaluated the results from different published sources and has harmonized estimates of lifecycle carbon emissions for electricity sources. Median estimates for natural gas technologies are greater than the 400 g CO_2e/kWh used in this simple example. See:

Garvin A. Heath, Patrick O'Donoughue, Douglas J. Arent, and Morgan Bazilian. "Harmonization of initial estimates of shale gas life cycle greenhouse gas emissions for electric power generation." *Proceedings of the National Academy of Science of the United States of America* (2014)

This means that a gas absorption heat pump will produce approximately 3 times greater emissions than the electric alternative for these assumptions (which are optimistic in favour of gas heat pump). Also note that this example did not consider the electrical consumption of the heat pump would which would increase emissions even further.

The example shows that the GHP would result in a significant increase in emissions in cooling mode for the jurisdictions considered in this study. Depending on the relative size of the heating and cooling loads, the cooling mode emissions increases could entirely negate any heating mode emissions reductions. As a technology for cost-effective emissions reductions, the non-reversible version (GAHP-A) is preferred in the Canada. Cooling mode operation was not evaluated further in this report. Note that renewable natural gas (RNG) would significantly impact this analysis but it was not considered because, at present, RNG is not a significant component of the natural gas supply.

10.6 Summary

The results presented in this section demonstrate that DHW pre-heating is the ideal application for this technology. Potential cost savings and carbon reductions are very attractive for DHW pre-heating because it exploits many factors contributing to a high-efficiency, chiefly: lower return temperatures, warmer outdoor ambient conditions for part of the year, potential to achieve greater operating hours, and reduced cycling losses.

11.0 BUSINESS CASE

The current Canadian distributor suggests that the list price of the GAHP-AR is approximately $25,000 (all dollar values are presented in Canadian dollars) and that for the non-reversible GAHP-A is $21,000 (both as of October 2018). The distributor also sells comparably-sized high-efficiency condensing boilers for $6,500. It follows that the incremental capital cost for the GAHP-A over a high-efficiency condensing boiler is currently estimated at approximately $14,500. However, note that the market for this technology in Canada is not mature and prices may come down as uptake increases.

The estimated annual net savings for DHW pre-heating applications in Toronto was approximately $1,500. If the GHP was able to benefit from carbon pricing program the additional savings is approximately $800 per year at $50 per ton of carbon. It follows that annual savings in the range of $1,500 to $2,300 may be achievable, resulting in a simple payback between 6 and 10 years.

It should be noted that carbon and cost savings varies drastically with the application and the climate. Space heating and DHW boiler replacement applications have much lower net savings because they are missing some important factors for achieving a high-efficiency.

Lower net cost savings would be less of a significant barrier if the incremental capital cost was not so large. The GHP costs three times more than a high-efficiency boiler base case and this factor may limit potential applications to those with very high annual net cost savings.

12.0 IMPLEMENTATION CONSIDERATIONS

When it was not used for testing, the GHP operated to meet the heating and cooling requirements of the ASH Lab. It operated without issue for the study period, which included both extremely cold and extremely hot temperatures. It did not require any special expertise over-and-above that required for the installation of any hydronic-based natural gas heating system. It is currently available (September 2018) via a Canadian distributor. Apartment-sized gas heat pump are available in Europe but not currently available in Canada.

13.0 OPPORTUNITIES FOR IMPROVEMENT

Figure 10-9 illustrated that a high efficiency is key for the cost-performance of this technology because the natural gas savings must be much greater than additional cost of the electricity required to run the heat pump. It follows that any factor that can further promote the efficiency of the heat pump, to push it into the territory of greater net cost savings, is of interest.

One factor inhibiting the efficiency of the heat pump in this study is the 50% propylene glycol used as a heat transfer fluid. This solution protects the equipment from damage due to freezing down to an ambient outdoor temperature of -34 °C but it also degrades efficiency. It would be possible to use a glycol solution with a lower concentration, but the gain in efficiency would be at the cost of an increased risk of damage to the equipment. It is at the discretion of the prospective system owner or system designer to decide if the gain in efficiency is worth the increased risk. However, the installation manual is unequivocal about the fact that the units must be protected to the lowest expected ambient temperature in the region installed.

One potential solution to maintain freeze protection while bolstering heat transfer properties is to use certain additives to the propylene glycol which promote the heat transfer properties of the fluid. This is the subject of a follow-up research project being conducted by the research team.

14.0 CONCLUSION

Gas heat pumps can obtain higher efficiencies than conventional gas heating equipment under many operating conditions. The key benefit of a gas heat pump over an electric heat pump is that it utilizes a low-cost fuel. This results in a better business case for certain applications and may ultimately promote wider-scale deployment and greater carbon emission reductions overall in the near-term.

While gas heat pumps are more commonly deployed in Europe or Japan, there is limited experience in North America, particularly in cold climates. To address this barrier, this study sought to evaluate the cold-climate performance of a gas absorption heat pump and determine the impact of certain key factors on heat pump performance.

The heat pump was the GAHP-AR from Robur. It is a gas-driven air-to-water heat pump that provides both heating and cooling. Rated heating capacity and efficiency are 35.3 kW and 126% (HHV), respectively, and the unit can supply fluid up to a temperature of 60 °C. A non-reversible version of the technology (GAHP-A) is also available. The heating capacity of this heat pumps makes it well-suited to large homes, multi-unit residential and industrial-commercial-institutional (ICI) sectors.

The heat pump was evaluated during one year of operation at the Archetype Sustainable House Lab at Kortright in Vaughan, ON. During this time, experimental measurements of capacity and efficiency were taken for a variety of different conditions covering normal operations. This created a performance map that detailed the effect of various parameters on overall performance. This map was then applied to different representative loads and climate data, in the context of an hourly bin-analysis, to estimate annual performance and savings in Canadian applications.

The analysis showed that, while the GHP is most effective in milder climates, the climate may actually matter less than the application. DHW pre-heating applications hold the greatest potential. When compared to a high efficiency boiler, annual net cost savings were estimated at approximately $1,500 (in Toronto) considering gas savings and electrical energy increases, while neglecting any incentives, rebates or carbon pricing.

Carbon savings for this application were substantial, estimated at approximately 16 tons CO_2e/year. If the heat pump can benefit from carbon pricing then annual savings could increase to approximately $2,300 (at a price of $50 per ton). Given an estimated incremental capital cost of approximately $14,500, this could result in a 6 to 10 year payback. Savings were lower for other applications. Note that the market for this technology in Canada is not mature and the incremental capital cost may come down as uptake increases.

The technology comes in a reversible version (GAHP-AR), which provides gas-powered heating *and* cooling, and a non-reversible (GAHP-A) version, which is heating-only. This study evaluated the GAHP-AR. It found that cooling mode is several times less efficient than conventional electrically-driven cooling. This would generate substantially greater carbon emissions in cooling mode and it follows that the non-reversible GAHP-A is preferred in most Canadian applications.

The approach used in this study was sufficient to identify, at a high-level, the applications and locations where the heat pump is best applied, as well as provide estimates of potential savings. However, the authors acknowledge that additional modeling work, exploring different system configurations and design options for prototypes of buildings, may be needed to fully evaluate the benefits of this technology in detail.

Gas absorption heat pumps are a very promising technology. This study showed that, while it is not a cost-effective replacement for conventional gas heating technologies in *every* instance, DHW applications particularly have potential for notable operational savings as well as substantial carbon savings when operating in a cold Canadian climate.

Future work will examine additives to the propylene glycol which promote the heat transfer properties of the fluid while maintaining its freeze protection capabilities.

15.0 APPENDIX A: PERFORMANCE DERATE FOR 50% GLYCOL

The manufacturer table for capacity corrections associated with different glycol concentrations is shown in Figure 15-1. A 50% glycol solution is associated with a capacity factor multiplier of 0.878 (note that water would be 1.0 because it requires no correction). However, it is useful to note that this correction factor was determined when the return and supply glycol temperatures were 54 and 44 °F (12.2 and 6.7 °C), respectively. In other words, the correction applies to cold glycol when the unit is in cooling mode. It would be useful to explore how this capacity correction may change with the glycol temperature.

ROBUR
caring for the environment

GLYCOL FACTOR TABLES

The water circuit of all Robur absorption cooling and heating equipment must be freeze protected. These tables pertain to freeze protection when using Propylene and Ethylene Glycols.

Propylene Glycol Capacity Correction Factor Table

Percent Propylene Glycol	15%	20%	25%	30%	35%	40%	50%
Approximate Freezing Point In °F	24°	18°	15°	9°	5°	-5°	-30°
Capacity Factor Multiplier *	0.992	0.986	0.972	0.960	0.950	0.928	0.878
Pressure Drop Multiplier **	1.04	1.08	1.13	1.21	1.26	1.47	2.79

Ethylene Glycol Capacity Correction Factor Table

Percent Ethylene Glycol	10%	15%	20%	25%	30%	35%	40%
Approximate Freezing Point In °F	25°	21°	17°	11°	5°	0°	-10°
Capacity Factor Multiplier *	0.98	0.96	0.95	0.93	0.92	0.91	0.89
Pressure Drop Multiplier **	1.08	1.11	1.16	1.21	1.27	1.32	1.38

* At Standard ARI 590 conditions: 54°F entering fluid temperature, 44°F leaving fluid temperature, 95°F ambient temperature, 0.0005 Fouling.

Figure 15-1. Glycol correction table from distributor.

The heat transfer from the heat pump to the glycol working fluid depends on the physical characteristics of the heat exchanger itself and the properties of the fluid. The key fluid properties in regards to heat transfer are density, viscosity, specific heat capacity and thermal conductivity.

A dense fluid with a high specific heat capacity will be a better heat transfer fluid because it can "carry" more heat energy for a comparable fluid flow rate. High thermal conductivity is desired for obvious

reasons and a low viscosity is important because it will enhance convective heat transfer compared to more viscous fluids. In essence, a lower viscousity fluid can interact better with the interior surface area of the heat exchanger. When compared to water, 50% glycol is a worse heat transfer fluid because it can "carry" less heat energy, it has poorer thermal conductivity and it is more viscous.

However, it is worthwhile to note that the difference in the heat transfer properties between water and 50% glycol are exacerbated at cold temperatures. This is primarily because the viscousity of 50% propylene glycol increases much more rapidly as the glycol temperature decreases. Putting it another way, 50% propylene glycol becomes much more "water-like" in terms of its heat transfer properties at warmer fluid temperatures. It follows that a glycol capacity multiplier factor for the heating mode fluid temperatures occurring during the heating mode testing, where return glycol temperatures were 32, 40 or 48 °C, would be better than the value given in Figure 15-1.

With significant effort it would be possible to estimate the effect of glycol temperature on the capacity factor multiplier. A better approach would be to empirically determine it through additional testing but both of these approaches were beyond the scope of this study.

In the context of this study, the discussion must conclude by noting the following point: the *cooling mode* capacity modifier for 50% glycol is 0.878 but the *heating mode* capacity modifier factor is higher and would reside somewhere between 0.878 and 1.0, with insufficient data to determine a more precise value.

16.0 APPENDIX B: EXAMPLE OF STEADY-STATE TESTING DATA

Example steady-state testing data from one test is shown in Figure 16-1 to Figure 16-5. This was Test #40. It used a high flow rate and a return temperature of 32 °C. It took place on February 8th 2018 at around noon and lasted approximately an hour. The average outdoor temperature during the testing was -6.7 °C. It confirms that a steady-state was achieved. Comparable steady-states were achieved on the large majority of tests.

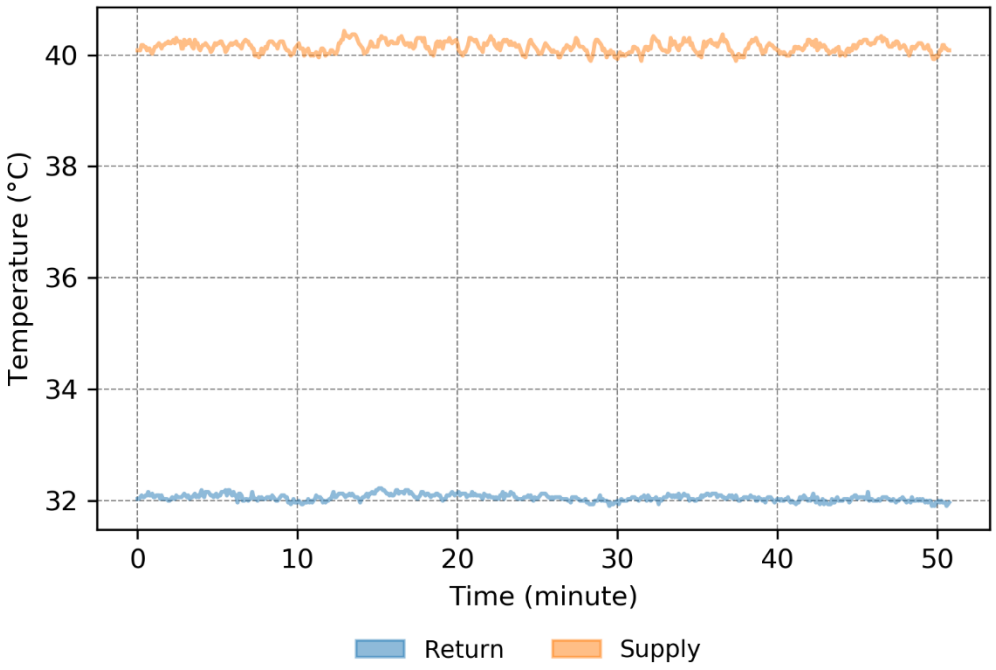

Figure 16-1. The supply and return temperatures to/from the GHP were kept in a steady-state by manually adjusting the variable auxiliary load.

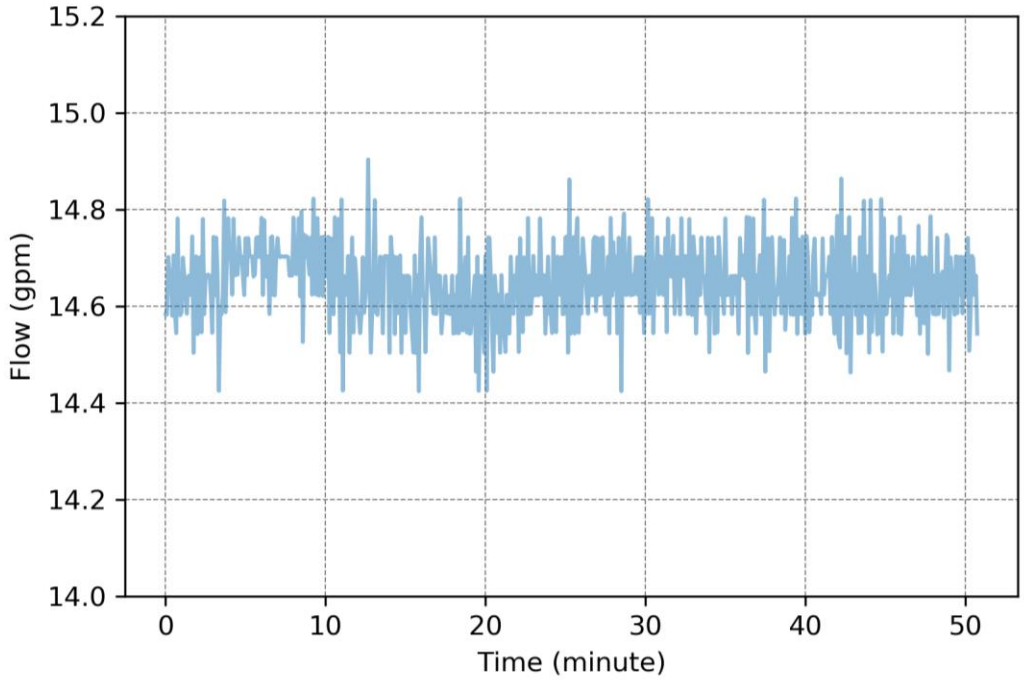

Figure 16-2. The pump was set at a constant speed throughout for the duration of the test.

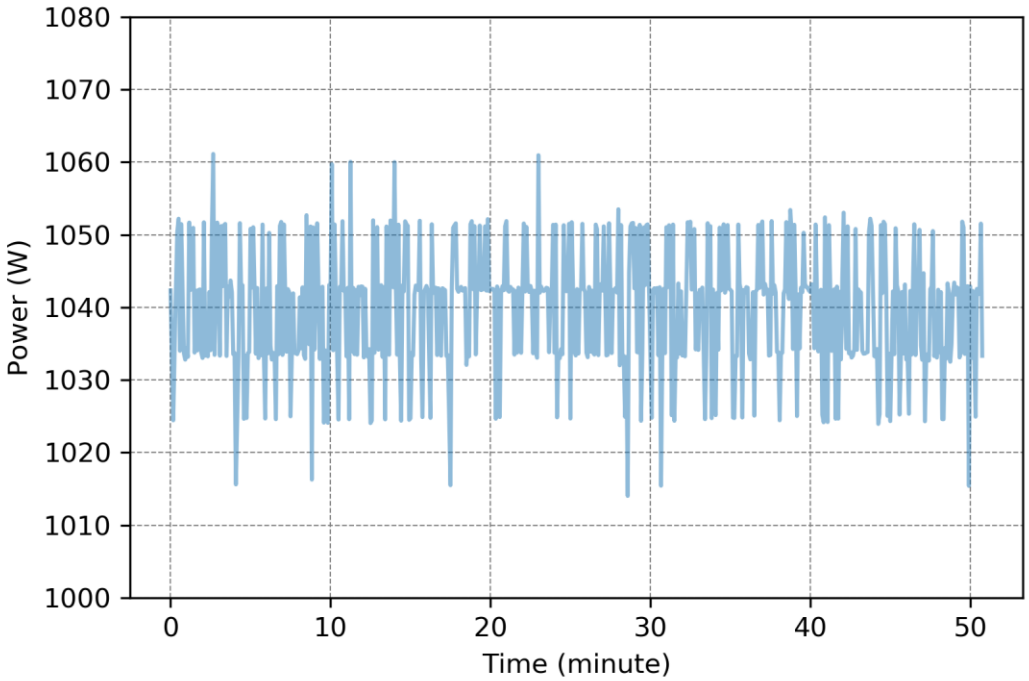

Figure 16-3. No significant fluctuations in power consumption were observed.

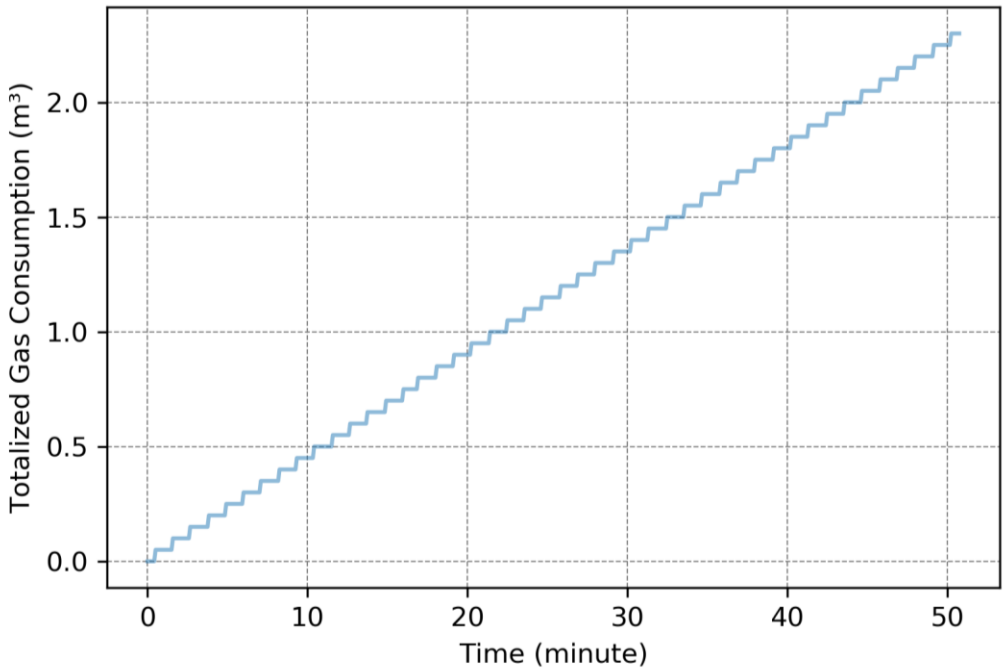

Figure 16-4. Gas consumption input was constant through the test.

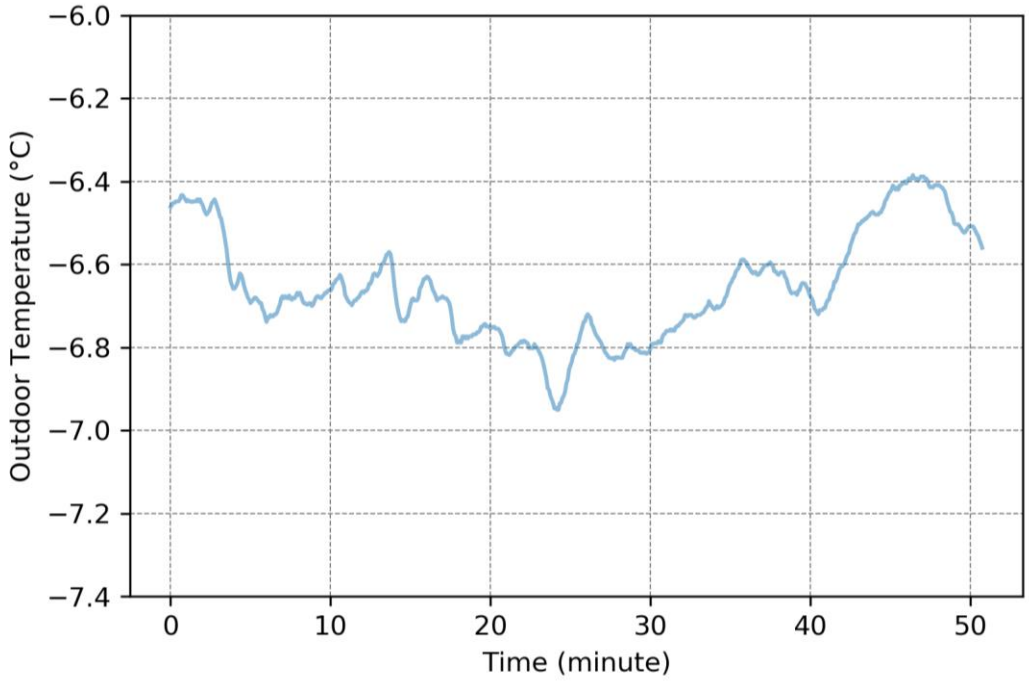

Figure 16-5. The outdoor temperate varied throughout the test between -6.4 and -7.0 °C, averaging -6.7 °C. This variable could not be controlled but given the short durations of the tests, typically less than an hour, the outdoor temperatures did not vary greatly.

17.0 APPENDIX C: SAMPLE ANNUAL PERFORMANCE CALCULATION

This sample calculation shows how annual efficiency and savings were calculated for one of the scenarios considered in this study: DHW pre-heating. Four functions needed to be defined:

- the efficiency curve $\eta(T)$,
- the capacity curve $\dot{q}(T)$,
- the load curve $L(T)$, and
- the frequency of hours versus outdoor temperature $n(T_i)$.

17.1 Capacity and Efficiency Curves

The scenario assumed that the return temperature was low, at 32ºC. The efficiency and capacity curves for a return temperature of 32 ˚C are presented in Figure 10-1 and Figure 10-2. The curves are explicitly defined below. It is based on a polynomial least squares regression of the experimental data. Recall that there was insufficient data at the endpoints to accurately define the curve – and the curve was simply set as a constant. The point at which the curve became a constant was chosen based on the local minima/maxima or saddle points of the polynomial fit that occurred near the endpoints. This ensured a continuous smooth function.

Efficiency for a 32 ˚C return was defined as:

$$-25.5 < T < 20.8: \quad \eta(T) = 2.101 \cdot 10^{-5} \cdot T^4 - 1.137 \cdot 10^{-3} \cdot T^3 - 3.122 \cdot 10^{-2} \cdot T^2 + 2.022 \cdot T + 1.138 \cdot 10^2$$

$$T < -25.5: \quad \eta(T) = \eta(-25.5)$$

$$T > 20.8: \quad \eta(T) = \eta(20.8)$$

Capacity for a 32 ˚C return was defined as:

$$-24.2 < T < 25.7 \quad \dot{q}(T) = 8.240 \cdot 10^{-6} \cdot T^4 - 2.981 \cdot 10^{-4} \cdot T^3 - 9.630 \cdot 10^{-3} \cdot T^2 + 5.383 \cdot 10^{-1} \cdot T + 3.124 \cdot 10^1$$

$$T < -24.2: \quad \dot{q}(T) = \eta(-24.2)$$

$$T > 25.7: \quad \dot{q}(T) = \eta(25.7)$$

17.2 Hourly Temperature Distribution

The frequency of hours versus outdoor temperature is shown in Figure 9-2 for Toronto. It is a discrete dataset rather than a continuous function.

17.3 Load Curve

For this scenario the load curve was equal to the capacity curve. Physically, this means that the GHP runs all the time.

17.4 Calculation

The calculation for annual efficiency and savings is shown in Table 17-1. The boiler efficiency was assumed to be 88%.

Table 17-1. Sample annual performance calculation for DHW pre-heating application in a Toronto.

T_i	$L(T_i)$	$n(T_i)$	$\eta(T_i)$	$\dot{q}(T_i)$	$L(T_i) \cdot n(T_i)$	$\frac{L(T_i) \cdot n(T_i)}{\eta_{Boiler}}$	$\frac{L(T_i) \cdot n(T_i)}{\eta(T_i)}$	$\left(\frac{L(T_i)}{\dot{q}(T_i)}\right) \cdot n(T_i)$
˚C	*kW*	*hours*	*%*	*kW*	*kWh (thermal)*	*kWh (thermal)*	*kWh (thermal)*	*hours*
-29.5	19.7	0	69.7	19.7	0.0	0.0	0.0	0
-28.5	19.7	0	69.7	19.7	0.0	0.0	0.0	0
-27.5	19.7	0	69.7	19.7	0.0	0.0	0.0	0
-26.5	19.7	0	69.7	19.7	0.0	0.0	0.0	0
-25.5	19.7	0	69.7	19.7	0.0	0.0	0.0	0
-24.5	19.7	0	69.8	19.7	0.0	0.0	0.0	0
-23.5	19.7	1	70.2	19.7	19.7	22.3	28.0	1
-22.5	19.8	5	70.8	19.8	98.8	112.3	139.5	5
-21.5	19.9	5	71.7	19.9	99.7	113.3	139.1	5
-20.5	20.2	5	72.7	20.2	100.9	114.7	138.7	5
-19.5	20.5	5	74.0	20.5	102.4	116.4	138.5	5
-18.5	20.8	8	75.4	20.8	166.7	189.4	221.2	8
-17.5	21.2	17	76.9	21.2	361.1	410.3	469.5	17
-16.5	21.7	15	78.6	21.7	325.3	369.7	413.8	15
-15.5	22.2	7	80.4	22.2	155.2	176.3	193.0	7
-14.5	22.7	21	82.3	22.7	476.3	541.3	578.7	21
-13.5	23.2	32	84.3	23.2	743.2	844.5	881.5	32
-12.5	23.8	53	86.4	23.8	1260.9	1432.8	1459.7	53
-11.5	24.4	52	88.5	24.4	1267.4	1440.3	1431.9	52
-10.5	25.0	82	90.7	25.0	2047.7	2326.9	2257.6	82
-9.5	25.6	80	92.9	25.6	2046.4	2325.4	2202.3	80
-8.5	26.2	125	95.2	26.2	3274.3	3720.8	3440.7	125
-7.5	26.8	116	97.4	26.8	3110.3	3534.4	3192.5	116
-6.5	27.4	148	99.7	27.4	4059.8	4613.4	4072.5	148
-5.5	28.0	167	101.9	28.0	4683.5	5322.2	4594.3	167
-4.5	28.7	158	104.2	28.7	4527.2	5144.5	4345.5	158

-3.5	29.3	150	106.4	29.3	4387.8	4986.1	4124.2	150
-2.5	29.8	200	108.6	29.8	5967.8	6781.6	5496.8	200
-1.5	30.4	200	110.7	30.4	6082.4	6911.8	5494.4	200
-0.5	31.0	249	112.8	31.0	7711.2	8762.7	6837.3	249
0.5	31.5	224	114.8	31.5	7057.5	8019.9	6147.5	224
1.5	32.0	206	116.8	32.0	6597.1	7496.7	5650.2	206
2.5	32.5	216	118.6	32.5	7024.6	7982.5	5920.8	216
3.5	33.0	232	120.4	33.0	7654.7	8698.6	6355.2	232
4.5	33.4	269	122.2	33.4	8996.3	10223.1	7363.7	269
5.5	33.9	277	123.8	33.9	9381.2	10660.5	7577.3	277
6.5	34.3	253	125.3	34.3	8669.0	9851.2	6915.9	253
7.5	34.6	233	126.8	34.6	8070.2	9170.6	6364.7	233
8.5	35.0	300	128.1	35.0	10493.9	11924.9	8189.2	300
9.5	35.3	272	129.4	35.3	9600.6	10909.8	7420.0	272
10.5	35.6	264	130.5	35.6	9394.6	10675.7	7197.4	264
11.5	35.8	274	131.6	35.8	9822.3	11161.6	7465.8	274
12.5	36.1	211	132.5	36.1	7613.5	8651.7	5746.5	211
13.5	36.3	199	133.3	36.3	7222.2	8207.0	5417.7	199
14.5	36.5	199	134.0	36.5	7258.7	8248.6	5416.3	199
15.5	36.6	223	134.6	36.6	8169.7	9283.8	6068.8	223
16.5	36.8	271	135.1	36.8	9965.2	11324.1	7375.4	271
17.5	36.9	330	135.5	36.9	12172.5	13832.3	8983.3	330
18.5	37.0	358	135.8	37.0	13239.0	15044.3	9750.0	358
19.5	37.1	334	136.0	37.1	12376.7	14064.5	9102.9	334
20.5	37.1	371	136.0	37.1	13769.8	15647.4	10121.4	371
21.5	37.2	311	136.0	37.2	11556.8	13132.7	8494.8	311
22.5	37.2	268	136.0	37.2	9967.7	11326.9	7326.7	268
23.5	37.2	197	136.0	37.2	7331.6	8331.4	5389.1	197
24.5	37.2	144	136.0	37.2	5361.5	6092.7	3941.0	144
25.5	37.2	135	136.0	37.2	5028.2	5713.9	3696.0	135
26.5	37.2	67	136.0	37.2	2495.5	2835.8	1834.3	67
27.5	37.2	61	136.0	37.2	2272.0	2581.8	1670.0	61
28.5	37.2	43	136.0	37.2	1601.6	1820.0	1177.2	43
29.5	37.2	39	136.0	37.2	1452.6	1650.7	1067.7	39
30.5	37.2	30	136.0	37.2	1117.4	1269.7	821.3	30
31.5	37.2	18	136.0	37.2	670.4	761.8	492.8	18
32.5	37.2	12	136.0	37.2	447.0	507.9	328.5	12
33.5	37.2	9	136.0	37.2	335.2	380.9	246.4	9
34.5	37.2	5	136.0	37.2	186.2	211.6	136.9	5
35.5	37.2	1	136.0	37.2	37.2	42.3	27.4	1

36.5	37.2	3	136.0	37.2	111.7	127.0	82.1	3
37.5	37.2	0	136.0	37.2	0.0	0.0	0.0	0
38.5	37.2	0	136.0	37.2	0.0	0.0	0.0	0
39.5	37.2	0	136.0	37.2	0.0	0.0	0.0	0
Totals:		**8,760**			**297,598**	**338,179**	**239,573**	**8,760**

The energy delivered to the load is 297,598 kWh (thermal). The gas energy required from the boiler or GHP to meet this load are 338,179 kWh (thermal) and 239,573 kWh (thermal), respectively.

The annual efficiency is:

$$\eta = \frac{297{,}598\ kWh}{239{,}573\ kWh} \cdot 100\% = 124\%$$

The annual gas energy savings is:

$$Q_{Savings} = 338{,}179\ kWh - 239{,}573\ kWh = 98{,}606\ kWh\ (thermal)$$

$$\frac{98{,}606\ kWh}{338{,}179\ kWh} \cdot 100\% = 29\%$$

The annual gas savings is:

$$S_{Gas} = \left(\frac{1\ m^3}{10.5\ kWh}\right) \cdot 98{,}606\ kWh = 9{,}391\ m^3$$

The annual electricity consumption is:

$$Q_{Elec} = 8{,}760\ hours\ \cdot 1.06\ kW = \ 9{,}286\ kWh\ (electrical)$$

The net cost savings is:

$$S_{Cost} = 9{,}391\ m^3 \cdot \left(0.30 \frac{\$}{m^3}\right) - 9{,}286\ kWh\ \cdot \left(0.14 \frac{\$}{kWh}\right) = 2{,}817\$ - 1{,}114\$ = 1{,}517\$$$

The net emissions savings is:

$$S_{Carbon} = 9{,}391\ m^3 \cdot \left(1.89\ \frac{kg\ eCO_2}{m^3}\right) - 9{,}286\ kWh\ \cdot \left(0.159 \frac{kg\ eCO_2}{kWh}\right)$$

$$= 17{,}749\ kg\ CO_2e - 1{,}476\ kg\ CO_2e$$

$$= 16{,}273\ kg\ CO_2e$$

18.0 APPENDIX D: IMPACT OF 50% PROPYLENE GLYCOL ON PERFORMANCE ESTIMATE FOR VANCOUVER

All performance projections presented in this report assumed that the heat transfer fluid was 50% propylene glycol because this was the fluid used during testing. Appendix A explained that this would degrade the performance when compared to water and also, that data was not available for the heating mode capacity modifier factor to understand the extent of the degradation.

The lack of this data is a moot point for Edmonton and Toronto because both would actually require a 50% propylene glycol heat transfer fluid for full freeze protection. However, Vancouver would not. A much lower concentration of glycol, or perhaps even water, may suffice. Figure 15-1 shows that even at 25% concentration, which provides freeze protection down to -8 °C, the effect of the glycol solution on performance is very small. It would be useful to gain a clearer understanding of how the results for Vancouver would be improved if a heat transfer fluid more appropriate for that climate were used.

Lack of data requires estimation of the heating mode capacity modifier factor. Two scenarios were considered. The first scenario assumed that the heating mode capacity modifier factor (CMF) for the 50% propylene glycol is 0.878, as given for cooling mode. This would produce a very optimistic estimate of performance. A second, likely more realistic scenario, estimated the heating mode capacity modifier factor at 0.95.

This was integrated into the calculation procedure by adjusting the efficiency and capacity curves. For simplicity, all curves for the different return temperatures were adjusted by the same amount. In the case of a heating mode CMF of 0.878, the curves were modified by a constant factor of 1.14 (i.e. 1/0.878). In the case of a heating mode CMF of 0.95, the curves were adjusted by a factor of 1.05.

The calculation procedure was then repeated for the adjusted efficiency/capacity curves in Vancouver. Results are shown in Figure 18-1. Under the assumption that there is no performance gain by switching from 50% propylene glycol to water in a Vancouver climate (CMF = 1.0), the annual savings does not deviate from the value of approximately $2,400 that was calculated in the body of the report. If there is a 5% efficiency gain by switching to water, then annual savings increases to $2,900 for the DHW pre-heat scenario. If there is a 14% efficiency gain by switching to water, then annual savings increases to $3,900 for the DHW pre-heat scenario. The former is likely a more realistic correction than the latter but regardless of the CMF assumed, the exercise demonstrates that Vancouver is an excellent climate for this technology.

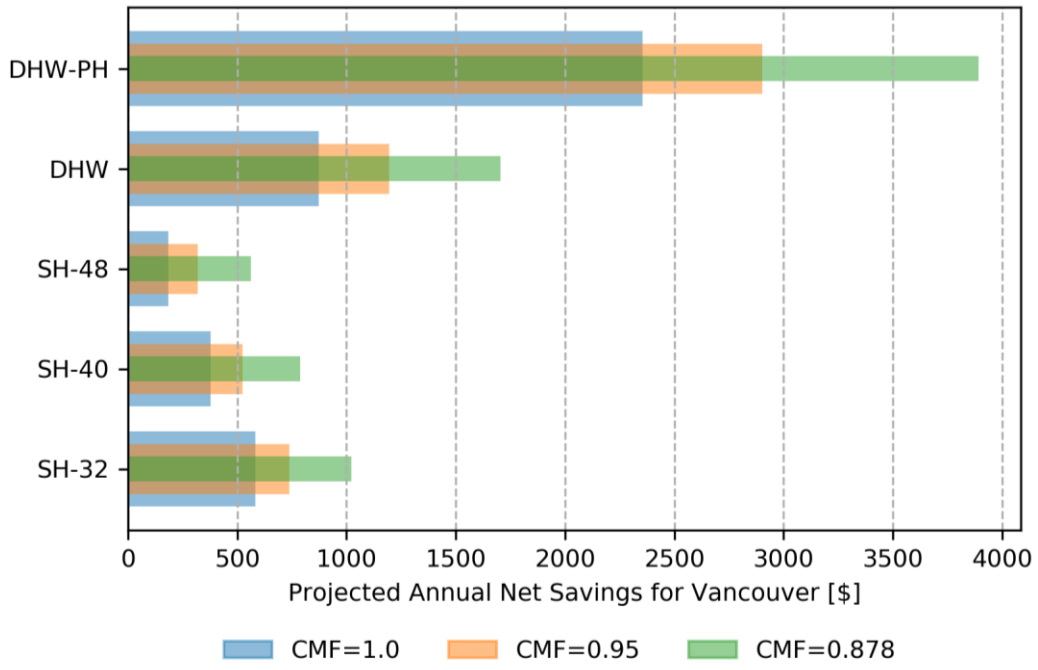

Figure 18-1. Annual net savings for different applications in Vancouver corrected for a water heat transfer fluid instead of propylene glycol. Different scenarios were considered since the capacity modifier factor for 50% propylene glycol in heating mode was not known.